



UNIVERSITY OF
GLOUCESTERSHIRE

This is a peer-reviewed, post-print (final draft post-refereeing) version of the following published document and is licensed under Creative Commons: Attribution-Noncommercial-No Derivative Works 4.0 license:

Brown, A G, Basell, L S and Toms, Phillip ORCID: 0000-0003-2149-046X (2015) A stacked Late Quaternary fluvio-periglacial sequence from the Axe valley, southern England with implications for landscape evolution and Palaeolithic archaeology. Quaternary Science Reviews, 116. pp. 106-121. doi:10.1016/j.quascirev.2015.02.016

Official URL: <http://dx.doi.org/10.1016/j.quascirev.2015.02.016>

DOI: <http://dx.doi.org/10.1016/j.quascirev.2015.02.016>

EPrint URI: <https://eprints.glos.ac.uk/id/eprint/3397>

Disclaimer

The University of Gloucestershire has obtained warranties from all depositors as to their title in the material deposited and as to their right to deposit such material.

The University of Gloucestershire makes no representation or warranties of commercial utility, title, or fitness for a particular purpose or any other warranty, express or implied in respect of any material deposited.

The University of Gloucestershire makes no representation that the use of the materials will not infringe any patent, copyright, trademark or other property or proprietary rights.

The University of Gloucestershire accepts no liability for any infringement of intellectual property rights in any material deposited but will remove such material from public view pending investigation in the event of an allegation of any such infringement.

PLEASE SCROLL DOWN FOR TEXT.

This is a peer-reviewed, post-print (final draft post-refereeing) version of the following published document:

Brown, A G and Basell, L S and Toms, Phillip (2015). *A stacked Late Quaternary fluvio-periglacial sequence from the Axe valley, southern England with implications for landscape evolution and Palaeolithic archaeology*. Quaternary Science Reviews, 116, 106-121. ISSN 02773791

Published in Quaternary Science Reviews, and available online at:

<http://www.sciencedirect.com/science/article/pii/S0277379115000967>

We recommend you cite the published (post-print) version.

The URL for the published version is

<http://dx.doi.org/10.1016/j.quascirev.2015.02.016>

Disclaimer

The University of Gloucestershire has obtained warranties from all depositors as to their title in the material deposited and as to their right to deposit such material.

The University of Gloucestershire makes no representation or warranties of commercial utility, title, or fitness for a particular purpose or any other warranty, express or implied in respect of any material deposited.

The University of Gloucestershire makes no representation that the use of the materials will not infringe any patent, copyright, trademark or other property or proprietary rights.

The University of Gloucestershire accepts no liability for any infringement of intellectual property rights in any material deposited but will remove such material from public view pending investigation in the event of an allegation of any such infringement.

PLEASE SCROLL DOWN FOR TEXT

1 **A stacked Late Quaternary fluvio-periglacial sequence from the Axe valley,**
2 **Southern England with implications for landscape evolution and Palaeolithic**
3 **archaeology**

4

5 A.G. Brown^{a,*}, L.S. Basell^b, P.S. Toms^c

6

7 ^{a*} Palaeoenvironmental Laboratory University of Southampton (PLUS), School of Geography, University
8 of Southampton, Highfields Campus, Southampton SO17 1BJ, United Kingdom. Tel. 02380 595493
9 Email: Tony.Brown@soton.ac.uk (corresponding author)

10 ^b Geography, Archaeology and Palaeoecology, Queen's University Belfast, Belfast BT71NN, United
11 Kingdom

12 ^c Luminescence dating laboratory, School of Natural and Social Sciences, University of Gloucestershire,
13 Swindon Road, Cheltenham GL50 4AZ, United Kingdom

14

15 **Abstract**

16 The current model of mid-latitudes late Quaternary gravel terrace sequences is that they are
17 uplift-driven but climatically controlled terrace staircases relate to both regional-scale crustal and
18 tectonic factors, and palaeohydrological variations forced by quasi-cyclic climatic catchment
19 conditions in the 100 K world (post Mid Pleistocene Transition). This model appears to hold for
20 the majority of the river valleys draining into the English Channel which exhibit 8-15 terrace
21 levels over approximately 60-100m of altitudinal elevation. However, one valley, the Axe, has
22 only one major morphological terrace and has long-been regarded as anomalous. This paper uses
23 both conventional and novel stratigraphical methods (digital granulometry and terrestrial laser
24 scanning) to show that this terrace is a stacked sedimentary sequence of 20-30m thickness with
25 a quasi-continuous (i.e. with hiatuses) pulsed, record of fluvial and periglacial sedimentation over
26 at least the last 300-400 K yrs as determined principally by OSL dating of the upper two thirds

27 of the sequence. Since uplift has been regional, there is no evidence of anomalous neotectonics,
28 and climatic history must be comparable to the adjacent catchments (both of which have staircase
29 sequences) a catchment-specific mechanism is required. The Axe is the only valley in North West
30 Europe incised entirely into the near-horizontally bedded chert (crypto-crystalline quartz) and
31 sand-rich Lower Cretaceous rocks creating a buried valley. Mapping of the valley slopes has
32 identified many large landslide scars associated with past and present springs. It is proposed that
33 these are thaw-slump scars and represent large hill-slope failures caused by Vauclausian water
34 pressures and hydraulic fracturing of the chert during rapid permafrost melting. A simple 1D
35 model of this thermokarstic process is used to explore this mechanism and it is proposed that the
36 resultant anomalously high input of chert and sand into the valley during terminations caused
37 pulsed aggradation until the last termination. It is also proposed that interglacial and interstadial
38 incision may have been prevented by the over-sized and interlocking nature of the sub-angular
39 chert clasts until the lateglacial when confinement of the river overcame this immobility
40 threshold. One result of this hydrogeologically mediated valley evolution was to provide a
41 sequence of proximal Palaeolithic archaeology over two MIS cycles. This study demonstrates
42 that uplift tectonics and climate alone do not fully determine Quaternary valley evolution and
43 that lithological and hydrogeological conditions are a fundamental cause of variation in terrestrial
44 Quaternary records and landform evolution.

45

46 **Keywords:** periglaciation, incision, chert, thermokarst, Quaternary hydrogeology, hydraulic
47 fracturing, bifaces, Palaeolithic, Acheulian

48

49

50

51 **1. Introduction**

52 The typical configuration of Quaternary fluvial sediment bodies along the NW border of Europe
53 is as river terrace staircases which decrease in age with decreasing altitude (Bridgland and
54 Westaway, 2007) as is seen in the Severn, and Thames (UK, Bridgland et al., 2004), Seine and
55 Somme (France; Antoine et al., 2000) and Middle Rhine (Germany; Westaway, 2002). This
56 scenario would be expected in non-cratonic areas where regional uplift has occurred (Bridgland
57 and Westaway, 2008). For example where, during the Quaternary, river systems are close to
58 glacial margins or within permafrost-affected regions and have been subject to large fluctuations
59 in sediment supply with or without uplift (Hancock and Anderson, 2002). Recent research and
60 sediment dating has shown that this model is frequently complicated by intra-cyclic sediments
61 forming compound terraces of two cold (stadial) phases (although rarely more) separated by
62 channel fills, loess or landsurfaces (e.g. palaeosols) of interstadial or interglacial origin (Lewin
63 and Gibbard, 2010). This staircase configuration is reversed below a hinge-line into subsiding
64 basins, such as the southern North Sea (Rhine) and into lateral diachroneity in tectonically stable
65 areas. Whilst this model was based upon the larger river systems in Europe it also holds for small
66 river systems and for most of the rivers along the coast of England (Brown et al., 2010) and
67 France which drain into the Channel River (English Channel/La Manche; Fig. 1a). The only
68 exception appears to be the River Axe which, as mapped by the British Geological Survey (BGS;
69 Edwards and Gallois, 2004), contains only one terrace at 14-30 m above the Holocene floodplain,
70 small (unmapped) fragments of a lower terrace only 1-2m above the floodplain and spreads of
71 'head' or solifluction gravels on the upper slopes (Fig. 2). These two gravel bodies make up the
72 Axe Valley Formation (Campbell et al., 1998a) which is known from three quarrying locations
73 Kilmington, Broom and Chard Junction Quarry (henceforth, CJQ). To the west the Otter and Exe
74 valleys (Fig. 1) have altitudinal staircases of 10 and 8 terraces respectively (Edwards and Gallois,
75 2004; Brown et al., 2009, 2010; Basell et al., 2011) and to the east the Frome/Piddle and Stour

76 systems (Fig. 1) also have altitudinal staircases of 12-15 terraces (BGS 2000) as would be
77 expected in a region that has undergone Quaternary regional-uplift (Westaway, 2010; 2011). The
78 River Axe is also known for a remarkably rich intra-fluvial Lower Palaeolithic site at Broom
79 (Reid Moir, 1936; Hosfield, 2008; Hosfield et al., 2011; Hosfield and Green, 2013) which has
80 produced over 1800 bifaces and is only comparable to rivers to the east at Woodgreen on the
81 River Avon, and Red Barns and Hill Head on the Solent River (Wenban-Smith and Hosfield,
82 2001). This paper presents the results of research at the only working quarry in the Axe valley
83 which had the aim of explaining this anomalous situation (i.e. single compound terrace) and
84 understanding its ramifications for both Quaternary landform evolution and Palaeolithic
85 archaeology.

86

87 **2. Previous Studies**

88 The Axe is one of several catchments which since the breaching of the Weald-Artois anticline,
89 have drained into the English Channel and southern North Sea but which lie just to the south of
90 the maximum glacial extent of the British-Irish-Fennoscandian ice sheet (Fig. 1) and experienced
91 periglacial conditions for most of the Late Quaternary (Mol et al., 2000; Renssen and
92 Vandenberghe 2003). The Quaternary evolution of the River Axe has received considerable
93 attention over the last 50 years due to its valley morphology and importance in Palaeolithic
94 archaeology. Its atypical nature (single terrace) was noted by Green (1974; 2013) and Shakesby
95 and Stephens (1984) and one of the aims of these studies was to test the hypothesis first proposed
96 by Mitchell (1960) and later by Stephens (1977) that the anomalously thick gravels resulted from
97 overflow through the Chard Gap (Fig. 3) from a ponded proglacial lake, Lake Maw, in the
98 Somerset Levels (Fig. 1). The gravels at Chard do not support this hypothesis for two reasons.
99 Firstly there are no clasts from the north Somerset area and secondly the gravels continue
100 upstream of the entry point of the Chard gap into the Axe Valley, and into upstream tributaries

101 (Green, 1974; Campbell et al., 1998; Green, 2013). What is certain from these studies is that the
102 Axe Valley and CJQ contains only one major morphological terrace and an anomalously thick
103 sequence of locally derived gravels, principally Upper Greensand chert and flint. OSL dating at
104 Broom also showed that the sequence younged upwards and is therefore a stacked or vertically
105 aggraded gravel body of Late Pleistocene age (Hosfield et al., 2006, 2011). The quarry at Chard
106 Junction which has been operating since the 1950s has produced occasional finds of Palaeolithic
107 artefacts but these have been out of context (not in the gravel faces) such as the twisted ovate
108 found by J. J. Wymer in 1959 and cordiform biface he also found in 1974. Wymer (1999) clearly
109 thought that the site had considerable potential probably due to its proximity to the well-known
110 sites at Broom (Hosfield et al., 2011; Hosfield and Green, 2013). Other than an isolated find out
111 of sedimentary context there has been no archaeological recording of the sub-surface archaeology
112 of the gravels at Chard Junction (Basell et al., 2007). Palaeolithic artefacts recorded in the county
113 Historic Environment Records (HERs) supplemented by museum records were plotted onto the
114 DEM/geology drape and it can be seen that there is a cluster of 11 in the CJQ area prior to this
115 study (Fig. 2).

116

117 **3. Catchment hydrogeology**

118 The bedrock geology and hydrogeology of the Axe valley are of critical importance to its
119 Quaternary evolution and so will be discussed in some detail. The English Channel cuts
120 discordantly across the Cenozoic basins and axial structures (anticlines) that run from the Seine
121 Basin to the Thames Basin and further west to the Wessex basin and Dorset plateaux (Fig. 1).
122 This provides the well-known laterally time-transgressive Mesozoic section that is known as the
123 Jurassic Coast. This mega-section youngs from the Upper Triassic at the west end (Exmouth
124 Sandstone and Mudstone) to the Upper Cretaceous at the east end (Upper Chalk Group). The
125 Axe catchment is located approximately mid-way along this sequence and is incised into a short

126 outcropping section of mid-Cretaceous Upper Greensand and chalk which form the scarp slopes
127 of the Blackdown Hills (Fig. 1c). The Upper Greensand is a sub-horizontal sequence of clays,
128 weakly- and un-cemented sandstones, and tabular chert overlain by clay-with-flints of Eocene
129 age. Large blocks of siliceous rock known as sarsens, are also found on the Blackdown plateau
130 and it is believed that they are also of Eocene age along with the clay-with-flints formation (Isaac,
131 1979; Scrivener et al., 2011). The valley has incised through this sequence and is now floored by
132 mudstones of Lower Jurassic age up to just above CJQ at Forde Abbey. This coincides with a
133 nick-point at the upper end of the incised valley (Fig. 3) with the result that the valley-sides below
134 this point are composed of a 120m thick ‘layer-cake’ of clay, sands and chert, sand and a basal
135 mudstone of low permeability. In contrast the catchments to the west are underlain by only
136 sandstones and mudstones (no chert) and to the east by chalk or Palaeogene sediments. A
137 particularly unusual feature is the sand-chert-sand alternation which occurs in the CJQ area at 90
138 to 160 m OD (m above ordnance datum sea level) and which produces a lower and upper spring-
139 line at the base of the two sandstone members (Foxmould Member and Bindon Sandstone
140 Member, Fig. 1). These members are separated by mineralised erosion surfaces (hardground)
141 forming hydrogeological discontinuities. Today minor seepage occurs from the upper spring-line
142 but the lower spring-line has historically had enough discharge to power a number of mills and
143 a gravity driven fountain at Forde Abbey. The chert is well exposed 5 km to the east of the Axe
144 valley at Shapwick/Pinhay Quarry where it is a 30m thick bed of cryptocrystalline silicate
145 fractured into tabular bedded blocks along the bedding which varies from 1cm to 40cm in
146 thickness (Eggerton Grit). The quarry also reveals large phreatic tubes towards the base of this
147 member (Brown et al., 2011a).

148

149 **4. Methodology**

150 The research at the recent extraction phases of CJQ (Hodge Ditch Phases I-III) was partly
151 designed to allow the testing of novel techniques with potential for the monitoring of difficult
152 Palaeolithic sites where there is a low density of lithic remains and an unknown potential for
153 environmental information (Brown et al., 2011b). To this end the study involved not only
154 standard lithological recording of gravel faces, but also geomorphological mapping, the analysis
155 of borehole and gamma cps logs, digital granulometry (DG) and terrestrial laser scanning (TLS).
156 Pre-extraction borehole records and gamma cps logs (Slatt et al., 1992) were used to derive a
157 stratigraphic cross-section of the terrace gravels at Hodge Ditch (Fig. 4). Although the
158 lithological descriptions did not reliably distinguish between the sandy gravels and other
159 diamictons it was found that matrix-rich diamicton had a consistently higher relative gamma cps
160 values (50+) allowing its differentiation from chert gravels and sands which both had low gamma
161 cps values (c. 10), due to the inherited mineralogy from the Eocene clays and the mudstones
162 (Brown et al, 2011b). The second novel methodological element of this project was the
163 application of DG. The method is common in the analysis of sediment thin sections and
164 geomorphology (Butler, et al. 2001; Graham et al. 2005a, 2005b; Strom et al. 2010) where it is
165 used for the determination of the grain size distribution of river gravels. The application here
166 uses a commercially available software (Sedimetrics®, Graham et al., 2005b) on vertical faces
167 of gravel to generate grain size distribution curves. A 10 mega pixels camera was used (Canon
168 Powershot 10XIS with a 20x optical zoom) give a minimum measurable grain size (MMGS) of
169 approximately 4 mm for a 0.3 m² frame area. Testing has shown that there is a linear relationship
170 between DG results and descriptive results derived from traditional sieving (Brown et al., 2011b;
171 Basell et al. subm.). The TLS system used was a Leica ScanStation HDS3000 at typical ranges
172 of 10-200m. A semi-permanent dGPS grid (using a Leica RX1250Xc GPS & GLONASS
173 SmartRover), was established with a network of 12 temporary benchmark (TBM) targets which
174 allowed any TLS position in the quarry to incorporate at least 3 reference targets. After

175 processing (including cleaning), registration using Leica GeoOffice Combined v7 x,y,z data were
176 exported and input into ArcGIS for solid model rendering used here and experimentally to
177 generate grain size data (Basell et al.subm.).

178
179 All the gravels investigated were fully decalcified due to the acidic nature of the majority of the
180 lithologies making up the catchment and so dating employed OSL initially as part of a wider
181 dating programme of South West British river deposits (Toms et al., 2008, 2013). For the OSL
182 dating, samples were collected in daylight from sections by means of opaque plastic tubing (150
183 x 45 mm) hammered into each face. In order to attain an intrinsic metric of reliability and where
184 possible, multiple samples were obtained from stratigraphically equivalent units targeting
185 positions likely to be divergent in dosimetry on the basis of textural differences. A measure of γ
186 dose rate was made in situ using an EG&G μ Nomad portable NaI gamma spectrometer. To
187 preclude optical erosion of the datable signal prior to measurement, all samples were prepared
188 under controlled laboratory illumination provided by Encapsulite RB-10 (red) filters. Following
189 segregation of material potentially exposed to light during sampling, fine sand sized quartz was
190 isolated by means of acid and alkaline digestion (10% HCl, 15% H₂O₂) to attain removal of
191 carbonate and organic components; a further acid digestion in HF (40%, 60 min) to etch the outer
192 10–15 mm layer affected by a radiation and degrade each samples' feldspar content; 10% HCl
193 was then added to remove acid soluble fluorides. Each sample was re-sieved and quartz isolated
194 from the remaining heavy mineral fraction using a sodium polytungstate density separation at
195 2.68 g cm³. Equivalent dose (D_e) values were acquired using a Risø TL-DA-15 irradiation-
196 stimulation-detection system (Markey et al., 1997; Bøtter-Jensen et al., 2003) and single-aliquot
197 regenerative dose protocol (Murray and Wintle, 2000; 2003). Optimal thermal treatment was
198 evaluated from measures of D_e and dose recovery preheat dependence. Dose rate (D_r) values
199 were estimated through a combination of *in situ* γ spectrometry (γD_r), Neutron Activation

200 Analysis (β Dr) and geographical position and overburden thickness (Cosmic Dr; Prescott and
201 Hutton, 1994). Disequilibrium in the U-series was monitored by means of *ex situ* gamma
202 spectrometry using an Ortec GEM-S high purity Ge coaxial detector system.

203

204 **5. Results: Stratigraphy, Sedimentology and Lithology**

205 Borehole logs reveal that the full sequence of deposits on the southern side of Hodge Ditch
206 extends from 79m to 47m OD at the thalweg of the buried valley although only the upper 23m
207 has been exposed by quarrying above the present water table. The general sequence across the
208 entire pit is typically tripartite above the mudstone bedrock head. A pit was dug in the quarry
209 floor to inspect the bedrock-sediment junction at c. 55m OD on the slope of the buried valley,
210 although boreholes indicate that the gravels extend to 47m OD. This pit revealed up to 1m of
211 highly fractured brecciated Charmouth Mudstone (Unit C, Fig. 4g) with a disrupted contact
212 exhibiting festoons and flame structures. Above the junction up to 64.4m OD are horizontally
213 bedded clast-supported medium to well sorted gravels, with occasional shallow cross-bedding
214 which includes trough-bedding varying between a SE to SW flow direction as would be expected
215 in braided river with a N-S orientated valley. Overlying these gravels is a thick but highly variable
216 unit of bedded fine to medium gravels (71-64.5m OD) with the development of large sand-filled
217 channels bisecting the site approximately from east to west. To the north and south the channel
218 is cut into horizontally bedded gravels. The sands display well-developed frost cracks (Fig. 4c),
219 micro-joints and normal faults with minor displacement (Grubbenvorst type *sensu* Mol et al.,
220 1993) and the gravels show features typical of cryoturbation including overturning, *in-situ*
221 shattered clasts and transported angular clasts of silty-sand. These deposits are highly laterally
222 variable as recorded by conventional logging (Fig. 4) and ground laser scanning (Fig. 5). At one
223 location in Hodge Ditch III a thin and reworked slightly organic clay palaeosol was observed
224 (Fig. 4b). Above an abrupt but irregular unconformity an upper matrix-rich, massive, poorly

225 sorted, dark-red gravel-rich diamicton formed the sloping superficial unit (unit A in Fig. 4) from
226 79m to 71m OD at its maximum thickness. This thins from the bedrock valley sides to the NE of
227 the site towards the valley axis. This unit has a high gamma cps values typical of a mixture of
228 the underlying weathered Lower Lias (including Charmouth Mudstones) and chert clasts. TLS
229 of 23 faces one of which is shown in Figure 5, were integrated and used to generate a solid model
230 (Fig. 6). Due to the high variability of the gravels both laterally and vertically only the sand
231 channel and the upper diamicton unit are differentiated in this model but it shows a former
232 channel of the Axe buried by renewed gravel deposition prior to the deposition of the palaeosol
233 (Fig. 4) and the diamicton.

234
235 Lithological analysis shows that the clasts throughout are overwhelmingly composed of sub-
236 rounded to angular chert typical of the Whitecliff Chert Member (70-80%) with 30-20% flint
237 although 0-2% of the clasts are quartz, quartzites and metamorphic rocks (Brown et al., 2011b).
238 Some of the chert clasts reach boulder size (>256mm long axis) and are typically sub-angular
239 with one or two faces showing a pre-weathered surface. This 'tabular' chert has probably been
240 derived from fractures and weathered scarp faces on the middle to upper valley-side slopes and
241 has undergone relatively little fluvial transport as the overwhelming majority of clasts were
242 angular to sub-angular (75-80%). The quartzites are all well rounded and originally derived from
243 Palaeozoic sources to the west later incorporated into a conglomerate within the Upper
244 Greensand cherts at Snowdon Quarries, near Chard, or the Trias Pebble Beds (Budleigh Salterton
245 Pebble Beds) which outcrop immediately to the west of the present Axe catchment. Alternatively
246 they could have been derived from an upper plateau gravel. Support for this origin comes from
247 the occurrence of some large pebbles and small boulders with thick grey weathering rinds,
248 solution pits and the occurrence at the site of occasional small 'sarsens' which are blocks of
249 silicified sandstone (silcretes) found on the Blackdown Plateau (Fig. 4). The grain size envelope

250 reveals the gravels beds to be very poorly sorted medium gravels to cobbles with a secondary
251 mode in the medium-coarse sand sized fraction (-1 phi). The lithic artefacts all fall into the upper
252 part of the range but none lie outside the D₉₅ of the gravel beds. However, the small sarsens lie
253 well outside the gravel range and are therefore very unlikely to have been transported into the
254 reach by fluvial processes. Although the bifaces are within the transported size-ranges their
255 condition varied from rolled (highly abraded) to fresh (unabraded with sharp edges).

256

257 **6. Results: archaeology and dating**

258 As part of the ad-hoc monitoring in 2008 two lanceolate bifaces were discovered (2°55'21" W
259 50°50'17" N) in close proximity and from the basal strata of the Hodge Ditch Phase I extraction
260 area (Brown and Basell, 2008). During continued recording of the site a further biface was found
261 during 2008. Further finds included a biface (broken in antiquity), a very small biface (found in
262 2013), a flake and a core in Hodge Ditch Phase II. Although none of these finds were discovered
263 embedded in a gravel face) they can all be confidently associated with specific areas and
264 stratigraphic units within the pit (Hodge Ditch II) and particular working levels at or below 56m
265 OD. They have been found on the southern areas of Hodge Ditch I and II and within the lower
266 gravels. These lithics vary from fresh with sharp edges, to moderately rolled and one is unusually
267 large (22 cm length and 1.1 kg in weight) suggesting two-handed use, probably for the butchery
268 of large herbivore carcasses (Schick and Toth, 1993). Given the large quantity of gravels removed
269 from Hodge Ditch I-III (over 1.8 M tons) and frequent monitoring throughout this represents a
270 low 'background' density probably related to hominin activity along the floodplain and at the
271 nearby high concentration site at Broom (Hosfield and Green, 2013).

272

273 Thirty three optical age estimates from Hodge Ditch I are outlined in Table 1 and illustrated in
274 Fig. 7. All but four samples (GL08047, GL09117, GL09118, GL10066) have D_e values of less

275 than 600 Gy, the maximum dose so far verified to produce accurate age estimates in the UK
276 (Pawley et al., 2010). Excluding those samples that failed analytical diagnostics (Table 1 and
277 Fig. 7), sedimentation between 55.8m and 66.5m OD appears centred upon a geometric mean
278 age of 259 ± 10 ka (MIS 7) but samples associated with the artefact level (GL08043, GL08044,
279 GL08046 but excluding GL08047) show convergent age estimates from divergent dosimetry
280 (Toms et al., 2005) providing an intrinsic measure of reliability and a weighted mean age of 326
281 ± 22 ka (MIS 9) but this should be considered as a minimum estimate for artefact age.

282
283 Additional dating evidence came from an exposure in Hodge Ditch III in 2011 when quarrying
284 revealed a small lens of dark-grey clay with associated mottling of the underlying sands at 0.8m
285 below the junction with the superficial diamicton. Analysis of the lens revealed it to be a low
286 organic content sandy silty-clay with unidentified small rootlets. Its thinness (1-4 cm) and the
287 minimal soil formation below it (no B horizon), suggest it is a re-worked organic channel fill.
288 Pollen analysis was undertaken on one large sample (100g) and despite the low sample counts
289 (Table 2) it is clear that the assemblage is dominated by tree pollen and particularly *Alnus*. The
290 presence of *Alnus* and other thermophilous trees (*Quercus*, *Fraxinus* and *Corylus*) clearly
291 indicates that this is from an interglacial rather than an interstadial and the presence of *Carpinus*
292 and *Taxus* and the sedimentary context below the upper diamicton unit the most likely ascription
293 is to some time in MIS5 and most likely 5e. The retained fraction from sieving produced very
294 little organic residue and no insect (coleoptera, diptera or chironomid) remains were found. The
295 plant material consisted only of unidentified fine root or stem material probably of
296 monocotyledonous origin, black humic matter and very small lignified fragments of stem. Some
297 small fragments of charcoal were present (under 2mm) and material including a few whole leaves
298 of bryophytes. Comparison with type material and reference to Smith (2004) showed them to be
299 typical of *Sphagnum* sp.. Studies using an environmental scanning electron (ESEM) revealed

300 chains of cubic crystals within carbonised plant tissues within a predominantly quartz matrix.
301 The individual crystals are 0.5-1 micron in size and typical of magnetotactic bacteria that require
302 molecular oxygen to produce magnetic minerals intracellularly in the form of a chain within a
303 magnetosome (Stolz et al., 1990). Microbial activity under conditions of low and alternating
304 redox potential is known to produce both spherules (Ariztegui and Dobson 1996; Brown et al.
305 2010) and chains (Stolz et al., 1990). Given the lack of soil structure and no B horizon, the
306 carbonised rootlets and the evidence of reducing conditions from the magnetobacteria we
307 conclude that this is the remains of a shallow pool or pond smeared-out probably by the
308 deposition of the overlying sand and gravel and possibly the deposition of the superficial
309 diamicton. It illustrates that there was a hiatus in floodplain aggradation and the floodplain
310 supported at least herbaceous vegetation growing in shallow pools during the last interglacial.

311

312 **7. Discussion: Geomorphological mapping and thermokarst formation**

313 This and other studies in the Axe valley have shown that the vast majority of the compound
314 terrace is locally derived chert from the Whitecliff Member and sand from the Greensand
315 Members (Foxmould and Bindon Sandstone) which outcrop on the valley sides (Fig. 1). Given
316 the thickness of gravels over a reach of approximately 25 km and the stratigraphy of the
317 superficial diamicton geomorphological mapping was undertaken in order to identify proximal
318 chert sources. An area of 6 km² upslope of the diamicton cone and the Hewood Bottom tributary
319 was mapped (Fig. 9). The valley-side slope above the quarry (NW corner of Fig. 9) which has an
320 average gradient (0.015 m m⁻¹), has a structurally controlled form reflecting the near horizontal
321 clay-with-flints, sandstone and chert stratigraphy. This produces an upper plateau, shallow ridges
322 and convex slopes, and lower chert-underlain rectilinear or concave slopes with alternating spurs
323 and shallow valleys. Descending from the springs along these valleys are a series of steep sided
324 gullies many of which have pronounced concave headwalls at or below the springs. These

325 features (Fig. 9 A-E) have arcuate to horseshoe-shaped planforms and are amphitheatre-like. The
 326 most pronounced which is located at the lower spring-line is 187 m across and 5 m deep. They
 327 are easily distinguished from quarries by their regular bowl-shape and locations on spring-lines.
 328 These features are remarkably similar to the scars left by ground-ice slumps or retrogressive
 329 thaw-slumps in areas undergoing rapid permafrost melting (Lewkowicz, 1988; Froese et al.,
 330 2008) such as the well-studied examples in the Yukon (Lantuit et al., 2012) (Fig. 9). Active
 331 retrogressive thaw-slumps consist of a steep (20°–90°) headwall of ice-rich permafrost and a
 332 more gentle (3°–10°) foot slope of thawed rock and soil (Burn and Lewkowicz, 1990) and in
 333 planform they can vary from open-arcuate/D shape to lemniscate/teardrop shape. These
 334 slumps would have fed a slurry of sand and chert directly onto the floodplain via the tributary.

335 Following from the identification of these features along with many indications of periglacial
 336 conditions affecting the palaeo-floodplain, it was decided to examine the implications of simple
 337 permafrost melt model on these slopes. In order to keep the model requirements as minimal as
 338 possible the model used was the simple surface temperature driven TTOP model (Fig. 10) from
 339 Wright et al. (2003):

340

$$341 \quad TTOP = \frac{K_t K_f (n_t DDT - n_f DDF)}{P} \quad \text{Eqn. 1}$$

342

343

344 Where TTOP is the temperature (°C) at the top of the permafrost, K_t is the thermal conductivity
 345 of the unfrozen ground, K_f is the thermal conductivity of the frozen ground, DDT is the air
 346 thawing index (degree days), DDF is the air freezing index (degree days), n_t is the thawing n-
 347 factor (vegetation), n_f is the freezing n-factor (vegetation) and P is the annual period (365 days).

348 From the estimation of TTOP and assuming a linear profile (so assuming a homogenous substrate

349 at that point on the slope) an estimate of permafrost thickness can be calculated by extrapolating
350 along the geothermal gradient to 0°C. The values used were taken from Lebret et al. (1994) for
351 K_t and K_f but with no correction for soil mineralogy as this has been found to be insignificant in
352 its effect (Riseborough and Smith, 1998). The values used are given in Table 3 and the surface
353 vegetation was assumed to be tundra. TTOP was generated from the estimated mean annual
354 temperature for southern England during the late glacial maximum (Atkinson et al. 1987) and a
355 sinusoidal annual temperature amplitude of 26°C which is slightly higher than a typical value for
356 modern arctic Canada (23°, Wright et al., 2003). When applied using these values the result is a
357 winter permafrost thickness varying from 88m to 122m with lithology (greater on the chert and
358 mudstone and less on the clays and sands) and deep enough to freeze the entire sedimentary
359 sequence outcropping on the slopes (Table 3; Fig. 10). Thawing was rapid and would have been
360 fastest on the sands, and clay with flints, and with the deepening of the active layer the sand
361 members would have been saturated but vertical drainage would be prevented by the aquicludes
362 (impermeable rocks) and any remaining permafrost in the chert and mudstones. If thawing of
363 bedrock and soil ice releases water faster than it can drain porewater pressures will rise, effective
364 rock stress fall, and frictional strength is reduced (Morgenstern and Nixon, 1971; Harris et al.
365 1995). The result would high pore-water pressures within the sand units and the chert, and very
366 high seepage pressures at both the upper and lower spring-line. Given the impermeable nature of
367 the chert this may have caused hydraulic fracturing of the chert, reduced frictional strength and
368 induced slope failure. In other words, ideal conditions for thaw-slump generation at these points
369 on the slopes, with the resultant mass failure of sand and chert in the form of debris-flows and
370 slumps with shear planes in the lower saturated Foxmould sand over the Gault and Eype Clay.
371 Under this scenario the chert would be transported as coarse clasts within a saturated sand matrix
372 in non-Newtonian flows even on low slopes, here typically 1-2°. These debris flow injections
373 onto the floodplain (similar to the upper diamicton) were reworked and sorted by the river until

374 MIS 4-2 when the river was confined by the debris-cone on the north side of the floodplain and
375 incised through the gravel stack. Reworking of the debris flows must have taken place when the
376 surface was unfrozen including under interstadial and interglacial periods. This is a process-based
377 version of the 'fluvioperiglacial' models of both Castleden (1980), Bryant (1983) and Shakesby
378 and Stephens (1984) and explains the anomalous accumulation of gravels from the Upper
379 Greensand slopes down to the buried valley at the present river mouth (Fig. 3). A possible
380 alternative model could be active layer saturation causing the retrogressive thaw slumps during
381 full periglacial conditions, however, these be so located at the bedrock junctions and springs –
382 hence our view that the cause is melting of the permafrost at cold period terminations.

383

384 **8. Discussion: Terrace formation**

385 Combining the stratigraphy and the OSL dating we suggest that the uppermost unit at Chard
386 Junction Quarry is solifluction and thaw-slump derived debris-flow deposits which accumulated
387 during the Devensian post MIS 5a. The uppermost OSL dates on the underlying bedded sand and
388 gravel suggest accumulation during the early Devensian MIS 5a-d and an MIS 5e date for the
389 organic deposits is consistent with the palynology. The middle bedded units of bed D appear to
390 have accumulated in cold stages MIS 6 and this is in agreement with the sedimentological
391 evidence of freezing of the floodplain surface. These sediments closely resemble the periglacial
392 alluviation model of Bryant (1983) with an abundant supply of sand and chert gravel deposited
393 as medial and lateral bars in a braided channel-system. The lowest accessible beds (i.e. those
394 above the present water table) may pre-date MIS 7 but confirmation of this is underway using
395 post-IR IRSL dating (Thomsen et al., 2008). The gravel-bedrock contact shows strong
396 development of brecciation which is interpreted here and elsewhere in southern England as being
397 due to permafrost ice-segregation and which made bedrock vulnerable to thermal erosion
398 (Murton and Lautridou, 2003; Murton and Belshaw, 2011). It follows that the incision of the

399 buried valley within which this sediment stack has accumulated was pre MIS 9-10 and given the
400 deep buried valley from CJQ to the coast it is most likely that it represents incision to the low
401 Mid-Pleistocene sea level during MIS 12 (Fig. 2). This accommodates additional incision of the
402 English Channel River due to breaching during at this time (Gupta et al., 2007). This does not
403 conform to the standard model (Bridgland and Westaway, 2007; Bridgland, 2000) and we suggest
404 this is because the Upper Greensand being highly erodible was deeply incised in the early
405 Pleistocene and incision, although slowed once the mudstones were encountered, was after MIS
406 12, prevented by sediment oversupply and the nature of the chert as bed material. It is also
407 possible that a threshold for incision reached after MIS 12 was not reached again until the
408 termination of the last glacial cycle.

409
410 This study has confirmed that the stone artefacts discovered at Chard come from the basal 10m
411 of the sequence and that the site has a low or background-level density, but that the lithics have
412 probably not travelled far from their point of discard. At Broom, and particularly the Ballast or
413 Railway Pit the stratigraphy and the archaeology differs significantly from that at Chard. In
414 particular at Broom there is the development of a laterally extensive pollen-bearing clays and
415 silts or a subaerial loam that was deposited in a temperate stage possibly during an interstadial
416 within MIS 8, or in MIS 9 (Hosfield et al., 2011; Hosfield and Green, 2013) and this is not the
417 case at CJQ which is a more active reach. The archaeology, which was an initial justification for
418 the study, is also different because the total number of finds from Chard is c. 23 (including local
419 surface finds), while Broom produced over 1800 stone tools. This study shows that this massive
420 difference is the result of a concentration of lithics at Broom probably due to nearby working of
421 chert vs low density probably discarded lithics at CJQ. Although the majority of the bifaces at
422 Broom are ovates and cordates, although pointed forms are known, the biface finds reported here
423 are similar being lanceolate (corresponding to Hosfield and Chamber's "pointed" categorization)

424 and cordate in form. Our research suggests that the biface-bearing gravels at CJQ are broadly
425 contemporaneous with the assemblage at Broom although at neither site has it been possible to
426 directly date a bed containing an *in-situ* artefact assemblage. This confirms that Broom is a
427 ‘super-site’ probably due to the reworking into the channel of a proximal archaeological context,
428 possibly even a biface pavement (Brown et al., 2013).

429
430 Taken together the sites at CJQ, Broom and Kilmington reveal episodic cold-stage
431 fluviperiglacial aggradation during the Middle-Late Pleistocene. In being a stacked sequence
432 the Axe Valley is exceptional in southern England and this requires explanation. The typical
433 geophysical context for terrace staircases is relative uplift with repeated down-cutting to low base
434 levels as provided by cold-period sea levels whereas stacked sequences are typical of subsiding
435 basins such as the lower Rhine sequence under the Netherlands (Peeters et al., 2014). Although
436 the area is affected by faults which may have been active into the Quaternary (Gallois, 2006)
437 there is no evidence that the Axe valley was part of a subsiding block relative to the catchments
438 each side of it. Indeed the whole Blackdown block, SW peninsula and South Coast has undergone
439 variable uplift during the Quaternary (Westaway, 2010; 2011). It is also self-evident that the
440 climate of this catchment must have been similar to its surrounding areas throughout the
441 Quaternary. An alternative explanation is that the catchment has, at some stage in the later
442 Quaternary, been reduced in size by river capture, thus reducing its discharge but not reducing
443 the sediment input from main valley slopes. Such a possibility has been postulated by Gallois
444 (2006) with capture of part of the adjacent proto-Otter by the Exe/Culm system but this did not
445 affect the Axe catchment. Shakesby and Stephens (1984) suggested that high rates of sediment
446 availability and periglacial transport produced the thickened Axe Valley Formation and Hosfield
447 and Green et al (2013) stress the erodible nature of the Upper Greensand lithologies. Whilst this
448 is undoubtedly correct we argue this is not enough, as similar conditions pertained in the adjacent

449 Otter Valley and the rivers draining the north and eastern edges of the Blackdown Plateau, all of
450 which exhibit terrace staircases. The mapping of the slopes above Chard Junction suggest that
451 the entire catchment was highly susceptible to thermokarstic melt-out processes at terminations
452 due fundamentally to its layered stratigraphy of highly permafrost-sensitive rocks i.e. sand with
453 fractured chert over a basal aquiclude. The pronounced spring-lines of the hills is seen largely as
454 a relic of the operation of a pressurised groundwater system during periglacial melting and
455 associated retrogressive thaw-slumping. Modelling has suggested that the occurrence of
456 pressurised groundwater systems was common in northwest Europe in areas of discontinuous
457 permafrost including river valleys and would have had its maximum effect in lithologies with
458 high effective porosities and permeabilities (van Weert et al., 1997).

459
460 The pre-fractured nature of the chert and the bimodal grain size of sediment (cobbles vs fine-
461 medium sand) may also be important for the lack of incision between stadials until the later
462 Devensian. The pre-fractured chert forms sub-angular blocks of cubic to tetrahedron shape which
463 after winnowing of the sand matrix have a tendency to lock together forming a pavement,
464 especially as upstream bedload input reduces (Dietrich et al., 1989). A simple calculation using
465 the grain size distribution envelope (Fig. 8) of the Shields stress required to move the D_{50} of the
466 gravels and the D_{95} suggests a 44% higher critical shear stress would be required to disrupt an
467 armoured bed and this takes no account of any imbrication and interlocking which would increase
468 this value further. Armouring and the thick gravel body would have increased hyporheic flow
469 during temperate conditions and reduced the likelihood of bed incision. This mechanism is
470 supported by the high lateral variability of the gravels formed as a result of laterally shifting
471 channels and bars and the common occurrence of small lenses of framework gravels. The
472 Devensian incision took place prior to the deposition of the lower inset terrace. Although not
473 dated in this study it is comparable in height and extent with the lowest terrace in the Exe system

474 which has been dated to the lateglacial stadial (Younger Dryas; Bennett et al., 2011). The sloping
475 surface of the terrace throughout the valley suggests the possibility that the solifluction/debris
476 flow unit was so extensive that it confined the channel to a small part of the floodplain. This
477 would have promoted incision when vegetation had stabilised valley slopes although this process
478 may have started as hyporheic in the depressed thaw zone under the floodplain under warming
479 climate conditions (Zarnetske, et al., 2008; Murton and Belshaw, 2011). This mechanism may
480 also provide an explanation for the prior incision of the valley floor which initiated the stacked
481 sequence post MIS 12 as suggested by the bedrock brecciation. It must also have been important
482 in increasing the erodibility of bedrock at floodplain edges thus facilitating lateral expansion of
483 the braidplain and what has been termed in the past fluvioperiglacial pedimentation *sensu*
484 Castleden (1980).

485

486 **10. Conclusions**

487 1. The chronostratigraphic data presented in this paper reveals that the Axe, a tributary valley of
488 the Channel River in southern England, has undergone quasi-continuous fluvial aggradation -
489 with hiatuses and lateral reworking - from MIS 10 and possibly MIS 12 until MIS 2 when it
490 underwent an incision and then a minor aggradational phase. The sediment-stack up to 32m in
491 total thickness is preserved in one major compound terrace with a sloping surface formed by
492 debris-flow deposits which is particularly well-developed at tributary junctions.

493 2. This morphology and developmental history is in stark contrast to all the other fluvial systems
494 draining into the English Channel/La Manche system in southern England and northern France
495 which are all terrace staircase systems regarded as typical of non-cratonic areas close to
496 Quaternary glacial margins. Such an anomaly requires an explanation within or outside the
497 current conceptual model of terrace formation. However, the Axe is also unusual in being entirely
498 incised into a near-horizontally bedded alternating sequence of weakly cemented sands and

499 cherts over mudstones of Mesozoic age. Geomorphological mapping of the valley slopes has
500 revealed features along prominent spring-lines which on morphological grounds are very similar
501 to modern retrogressive thaw slumps found in areas of melting permafrost.

502 3. A simple 1D model (TTOP) is used to test this hypothesis and it suggests that that permafrost
503 differentially melted in non-cemented sands both below and above the chert beds producing a
504 pressurised groundwater system which instigated hydraulic fracturing of the chert and
505 retrogressive thaw slumping. This liberated the pre-fractured chert in debris-flows providing a
506 high input of both sub-angular chert within fluidized sand onto the floodplain. This input was
507 locally reworked by fluvial activity but not incised into until the lateglacial. The reasons for this
508 change in fluvial behaviour are not known but may be due to a combination of the confinement
509 of the river by debris flow deposits and thermokarst induced down-cutting after reduced sediment
510 supply.

511 4. One result of this hydrogeologically mediated valley evolution was to provide a record of both
512 proximal (near-site) and background Lower Palaeolithic archaeological activity. The similarity
513 between the artifact typologies at CJQ and nearby Broom and the OSL dating at both sites
514 suggests a common age of either MIS 9 or 7, and the low-density of artefacts at CJQ confirms
515 the importance of Broom as a ‘super-site’ (*sensu* Ashton and Hosfield 2010 and Brown et al
516 2013) and its likely proximity to an *in-situ* assemblage reworked into an adjacent channel.

517 5. Most importantly this study demonstrates that uplift tectonics and climate alone do not fully
518 determine Quaternary valley evolution and that lithological and hydrogeological conditions are
519 a fundamental cause of variation in terrestrial Quaternary records.

520

521 **Acknowledgements**

522 The authors must thank all employees of Bardon Aggregates (Aggregate Industries Ltd.) who
523 have assisted this work in every possible way and in particular Tony Pearson, the site manager.

524 We must also thank Buzz Busby and Vanessa Straker of English Heritage for their help and
525 encouragement. The research was funded by English Heritage under grant Nos. PNUM 3847 and
526 5695. This work has benefited from both unpublished data and discussions with Rob Hosfield,
527 Chris Green, Rick Shakesby, Hugh Prudden and many members of the British Quaternary
528 Research Association visit to the site in 2011.

529

530

531 **References**

532 Antoine, P., Lautridou, J. P. and Laurent, M. 2000. Long-term archives in NW Europe: response
533 of the Seine and Somme rivers to tectonic movements, climatic variations and sea-level changes.
534 *Geomorphology* 33, 183-207.

535

536 Ariztegui, D., & Dobson, J., 1996. Magnetic investigations of framboidal greigite formation; a
537 record of anthropogenic environmental changes in eutrophic Lake St Moritz, Switzerland. *The*
538 *Holocene* 6, 235–241.

539

540 Ashton, N. M. and Hosfield, R. T. 2010. Mapping the human record in the British early
541 Palaeolithic: Evidence from the Solent river system. *Journal of Quaternary Science* 25, 737-753.

542

543 Atkinson, T.C., Briffa, K. R. and Cooper, G. R. 1987 Seasonal temperatures in Britain during
544 the past 22,000 years reconstructed using beetle evidence. *Nature* 325, 587-592.

545

546 Basell, L. S., Brown, A. G. and Hosfield, R. T. 2007. *The Palaeolithic Rivers of South-West*
547 *Britain (PNUM 3847). Fieldwork Report (Phase II)*. English Heritage, London/ADS York,
548 <http://www.personal.rdg.ac.uk/~sgs04rh/SWRivers/Fieldwork%20Report.pdf>

549

550 Basell, L.S., Brown, A. G. and Neild, J. (Subm.) The use of terrestrial laser scanning for the
551 monitoring and sedimentological investigations of an artefact-bearing fluvial sequence in
552 Southern England. *Journal of Archaeological Science*

553

554 Basell, L. S., Brown, A. G., Toms, P. S. and Gallois, R. 2011. The Otter valley gravels and
555 Budleigh Salterton. In L. S. Basell, A. G. Brown and P. S. Toms (Eds.) *The Quaternary of the*
556 *Exe Valley and Adjoining Area. Field Guide*. Quaternary Research Association, London, 139-
557 147.

558

559 Bennett, J. A., Brown, A. G. and Basell, L. S. 2011. Late Pleistocene and Holocene deposits in
560 the Netherex area. In L. S. Basell, A. G. Brown and P. S. Toms (Eds.) *The Quaternary of the*
561 *Exe Valley and Adjoining Area. Field Guide*. Quaternary Research Association, London, 67-76.

562

563 Bøtter-Jensen, L., McKeever, S.W.S. and Wintle, A.G. (2003) *Optically Stimulated*
564 *Luminescence Dosimetry*. Elsevier, Amsterdam.

565

566 Bridgland, D.R., 2000. River terrace systems in North West Europe: an archive of environmental
567 change, uplift and early human occupation. *Quaternary Science Reviews* 19, 1293–1303.

568

569 Bridgland, D. R. and Westaway, R. 2007. Climatically controlled river terrace staircases: a
570 worldwide Quaternary phenomenon. *Geomorphology* 98, 285-315.

571

572 Bridgland, D. R. and Westaway, R. 2008. Climatically controlled river terrace staircases: a
573 worldwide Quaternary phenomena. *Geomorphology* 98, 285-315.

574

575 Bridgland, D.R., Schreve, D.C., Keen, D.H., Meyrick, R., and Westaway, R., 2004.

576 Biostratigraphical correlation between the late Quaternary sequence of the Thames and key

577 fluvial localities in Central Germany. *Proceedings of the Geologists Association* 115, 125–140.

578

579 British Geological Survey. 2000. *Dorchester, England and wales Sheet 328. Solid and Drift,*

580 *1:50,000.* British Geological Survey, Keyworth, Nottingham.

581

582 Brown, A. G. and Basell, L. S. 2008. New Lower Palaeolithic finds from the Axe Valley, Dorset.

583 *PAST* 60, 1-4.

584

585 Brown, A. G., Ellis, C. and R. Roseff, R. 2010. Holocene sulphur-Rich palaeochannel sediments:

586 Diagenetic conditions, magnetic properties and archaeological implications. *J. of Archaeological*

587 *Science* 37, 21-29.

588

589 Brown, A. G., Basell, L. S., Toms, P. S. and Scrivner, R. C. 2009. Towards a budget approach to

590 Pleistocene terraces: preliminary studies using the River Exe in South West England.

591 *Proceedings of the Geologists' Association.* 120, 275-281.

592

593 Brown, A. G., Basell, L.S, Toms, P.S., Bennett, J., Hosfield, R.T. and Scrivener, R.C. 2010. Late

594 Pleistocene Evolution of the Exe Valley. A Chronstratigraphic Model of Terrace Formation and

595 its Implications for Palaeolithic Archaeology. *Quaternary Science Reviews* 29, 897-912.

596

597 Brown, A. G., Powell, M., and Basell, L. S. 2011a. Recent work at Shapwick Grange Quarry and

the Blackdown Hills Plateau. In L. S. Basell, A. G. Brown and P. S. Toms (Eds.) *The Quaternary*

598 *of the Exe Valley and Adjoining Area. Field Guide.* Quaternary Research Association, London,
599 128-132.

600 Brown, A. G., Toms, P. S. and Basell, L. S. 2011b. Monitoring and modelling of the Palaeolithic
601 archaeological resource at Chard Junction Quarry, Hodge Ditch Phases II & III. PNUM 5695.
602 English Heritage Report, ADS York.

603

604 Brown, A. G., Basell, L. S., Robinson, S. and . Burge, G. C. 2013. Site Distribution at the Edge
605 of the Palaeolithic World: A Nutritional Niche Approach. *PLoS ONE* 8(12), e81476, 1-14.

606

607 Bryant, I. D. 1983. Facies sequences associated with some braided river deposits of late
608 Pleistocene age from Southern Britain. In *Modern and ancient fluvial systems*. J. D. Collinson
609 and J. Lewin. Oxford, Blackwell Scientific Publications, 267-275.

610

611 Burn, C.R., and Lewkowicz, A.G. 1990. Retrogressive thaw slumps. *The Canadian Geographer*
612 34, 273–276.

613

614 Butler, J. B., S. N. Lane, and J. H. Chandler. 2001. Automated extraction of grain-size data from
615 gravel surfaces using digital image processing. *Journal of Hydraulic Research* 39, 519-529.

616

617 Campbell, S, Scourse, J.D., Hunt, C.O., Keen, D.H. and Stephens, N. 1998a. *Quaternary of*
618 *South-west England*. Geological Conservation Review Volume, Chapman and Hall, London.

619

620 Campbell, S., Stephens, N., Green, C.P. and Shakesby, R. A. 1998b. Broom gravel pits. In
621 *Quaternary of South-West England*, Campbell, S., Hunt, C.O., Scourse, J.D., Keen, D.H. and

622 Stephens, N. (eds). Geological Conservation Review series, Vol. 14 Chapman & Hall: London;
623 307–318.
624
625 Castleden, R., 1980. Fluvioglacial pedimentation: a general theory of fluvial valley development
626 in cool temperate lands, illustrated from western and central Europe. *Catena* 7, 135–152.
627
628 Dietrich, W. E., Kirchner, J. W., Ikeda, H. and Isega, H. 1989. Sediment supply and the
629 development of coarse surface layers in gravel-bedded rivers. *Nature* 340, 215-217.
630
631 Edwards, R.A. and Gallois, R. W. 2004. *A brief description of the geology of the Sidmouth*
632 *district. British Geological Survey Sheet Explanation. Sheets 326/340 (England and Wales)*
633
634 Froese, D. G., Estgate, J. A., Reyes, A., Enkin, R. J. and Preece, S. J. 2008. Ancient permafrost
635 and future, warmer Arctic. *Science* 321, 1648.
636
637 Gallois, R.W. 2006. The evolution of the rivers of east Devon and south Somerset, UK.
638 *Geoscience in south-west England* 11, 205-213.
639
640 Gardiner V. and Dackombe, R. 1983. *Geomorphological field manual*. George Allen & Unwin,
641 London.
642
643 Graham, D. J., Reid, I. and Rice, S. P. 2005a. Automated sizing of coarse-grained sediments:
644 image-processing procedures. *Mathematical Geology*, 37, 1-28.
645

646 Graham, D. J., Rice, S. P. and Reid, I. 2005b A transferable method for the automated grain
647 sizing of river gravels. *Water Resources Research* 41, 1-12.
648

649 Green, C. P. 1974. Pleistocene gravels of the River Axe in south-western England, and their
650 bearing on the southern limit of glaciation in Britain. *Geological Magazine* 111, 213-220.
651

652 Green, C.P. 2013. Broom and the Axe Valley in the Middle Pleistocene. In Hosfield, R. and
653 Green, C. P. (Eds.) *Quaternary History of Palaeolithic Archaeology in the Axe valley at Broom,*
654 *South West England.* Oxbow, Oxford, 165-169.
655

656 Gupta, S., Collier, J. S., Palmer-Felgate, A. and Potter, G. 2007. Catastrophic flooding origin of
657 shelf-valley systems in the English Channel. *Nature* 448, 342-345.
658

659 Hancock, G.S., Anderson, R.S., 2002. Numerical modelling of fluvial strath-terrace formation in
660 response to oscillating climate. *Geological Society of America Bulletin*, 114, 1131–1142.
661

662 Harris, C., Davies, M. C. R. and Coutard, J-P. 1995. Laboratory simulation of periglacial
663 solifluction: significance of porewater pressures, moisture contents and undrained shear strengths
664 during soil thawing. *Permafrost and Periglacial Processes* 6, 293-311.
665

666 Hosfield, R.T. 2008. Stability or flexibility? Handaxes and hominins in the Lower Palaeolithic.
667 In: Papagianni, D., Maschner, H. and Layton, R. (eds.) *Time and Change: Archaeological and*
668 *Anthropological Perspectives on the Long Term.* Oxbow Books, Oxford, 15-36.
669

670 Hosfield, R. and Green, C. P. (Eds.) 2013. *Quaternary History of Palaeolithic Archaeology in*
671 *the Axe valley at Broom, South West England*. Oxbow, Oxford.

672

673 Hosfield, R. T., Brown, A. G., Basell, L., Hounsell, S. and Young, R. 2006. *The Palaeolithic*
674 *Rivers of South-West Britain. Final Report Phases I & II*. English Heritage, London.

675 Hosfield, R. T., Green, C., Toms, P., Scourse, J. Scaife, R. and Chambers, J. 2011. The Middle
676 Pleistocene deposits and archaeology at Broom. In L. S. Basell, A. G. Brown and P. S. Toms
677 (Eds.) *The Quaternary of the Exe and Adjoining Areas. Field Guide*. Quaternary Research
678 Association, London, 103-127.

679

680 Isaac, K. P. 1979. Tertiary silcretes of the Sidmouth area, east Devon. *Proceedings of the Ussher*
681 *Society* 4, 341-354.

682

683 Lantuit, H., Pollard, W. H., Couture, N., Fritz, M., Meyer, H. and Hubberten, H-W. 2012. Modern
684 and late Holocene retrogressive thaw slump activity on the Yukon coastal plain and Herschel
685 Island, Yukon Territory, Canada. *Permafrost and Periglacial Processes* 23, 39-51.

686

687 Lebret, P., Dupas, A., Clet, M., Coutard, J-P., Lautridou, J-P., Courbouleix, S., Garcin, M. and
688 Levy, M. 1994. Modelling of permafrost thickness during the late glacial stage in France:
689 preliminary results. *Canadian Journal of earth Sciences* 31, 959-968.

690

691 Lewkowicz, A. G. 1988. Slope processes. In M. J. Clark (Ed.) *Advances in Periglacial*
692 *Geomorphology*, Wiley, Chichester 325-368.

693

694 Lewin, J. and Gibbard, P. 2010. Quaternary river terraces in England: Forms, sediments and
695 processes. *Geomorphology* 120, 293-311.

696 Markey, B.G., Bøtter-Jensen, L., and Duller, G.A.T. 1997. A new flexible system for measuring
697 thermally and optically stimulated luminescence. *Radiation Measurements*, 27, 83-89.

698

699 Mitchell, C. F. 1960. The Pleistocene history of the Irish Sea. *Advancement of Science*, 17, 313-
700 25.

701

702 Mol, J., Vandenberghe, J., Kasse, K. and Stel, H. 1993. Periglacial microjointing and faulting in
703 Weichselian fluvio-aeolian deposits. *Journal of Quaternary Science* 8, 15-30.

704

705 Mol, J., Vandenberghe, J., and Kasse, C. 2000. River response to variations of periglacial climate
706 in mid-latitude Europe. *Geomorphology* 33, 131-148.

707

708 Morgenstern, N. R. and Nixon, J. F. 1971. One dimensional consolidation of thawing soils.
709 *Canadian Geotechnical Journal* 11, 447-469.

710

711 Murray, A.S. and Wintle, A.G. 2000. Luminescence dating of quartz using an improved single-
712 aliquot regenerative-dose protocol. *Radiation Measurements*, 32, 57-73.

713

714 Murray, A.S. and Wintle, A.G. 2003. The single aliquot regenerative dose protocol: potential for
715 improvements in reliability. *Radiation Measurements*, 37, 377-381.

716

717 Murton, J. B. and Belshaw, R. K. 2011. A conceptual model of valley incision, planation and
718 terrace formation during cold and arid permafrost conditions of Pleistocene southern England.
719 *Quaternary Research* 75, 385-394.
720

721 Murton, J. B. and Lautridou, J-P., 2003. Recent advances in the understanding of Quaternary
722 periglacial features of the English Chanel coastlands. *Journal of Quaternary Science* 18, 301-
723 307.
724

725 Pawley, S.M., Toms, P.S., Armitage, S.J., Rose, J. (2010) Quartz luminescence dating of Anglian
726 Stage fluvial sediments: Comparison of SAR age estimates to the terrace chronology of the
727 Middle Thames valley, UK. *Quaternary Geochronology* 5, 569-582.
728

729 Peeters, J., Busschers, F.S. and Stouthamer, E. 2014. Fluvial evolution of the Rhine during the
730 last interglacial-glacial cycle in the southern North Sea basin: A review and look forward.
731 *Quaternary International*
732

733 Prescott, J.R. and Hutton, J.T. (1994) Cosmic ray contributions to dose rates for luminescence
734 and ESR dating: large depths and long-term time variations. *Radiation Measurements*, 23, 497-
735 500.
736

737 Reid Moir, J. 1936. Ancient Man in Devon. *Proceedings of the Devon Archaeological*
738 *Exploration Society* 2, 264-275.
739

740 Renssen, H. and Vandenberghe, J. 2003. Investigation of the relationship between permafrost
741 distribution in NW Europe and extensive winter-sea ice cover in the North Atlantic Ocean during
742 the cold phases of the last Glaciation. *Quaternary Science Reviews* 22, 209-223.
743

744 Riseborough, D. W. and Smith, M. W. 1998. Exploring the limits of permafrost. In A. G.
745 Lewkowicz and M. Allard (Eds.), *Permafrost: Seventh International Conference, Yellowknife,*
746 *Canada*, 935-942.
747

748 Scrivener, R. C., Basell, L. S. and Brown, A. G. 2011. Sarsens associated with river terrace
749 gravels in the Creedy valley, Devon. In L. S. Basell, A. G. Brown and P. S. Toms (Eds.) *The*
750 *Quaternary of the Exe Valley and Adjoining Area. Field Guide.* Quaternary Research
751 Association, London, 128-132.
752

753 Schick, K. and Toth, N. 1993. *Making Silent Stones Speak: Human Evolution and the Dawn of*
754 *Technology.* Simon & Schuster, New York.
755

756 Shakesby, R. A. and Stephens, N. 1984. The Pleistocene gravels of the Axe Valley, Devon.
757 *Report of the Transactions of the Devon Association for the Advancement for Science* 116, 77-
758 88.
759

760 Slatt, R. M., Jordan, D. W., D'Agostino, A. E. & Gillespie, R. H. 1992 Outcrop gamma-ray
761 logging to improve understanding of subsurface well log correlations. *Geological Society,*
762 *London, Special Publications* 65, 3-19.
763

764 Smith, A. J. E. 2004. *The Moss Flora of Britain and Ireland. Second Edition.* Cambridge
765 University Press, Cambridge.
766

767 Stephens, N. 1977. The Axe Valley. In D. N. Mottishead (Ed.) *INQUA Congress Guidebook for*
768 *Excursions A6 and C6. South-west England.* Geo Abstracts, Norwich, 24-29.
769

770 Stolz, J.F., Lovley, D.N., Haggerty, S.E., 1990. Biogenic magnetite and the magnetisation of
771 sediments. *Journal of Geophysical Research* 95, 4355–4361.
772

773 Strom, K. B., Kuhns, R. D. & Lucas, H. J. 2010. Comparison of automated image-based grain
774 sizing to standard pebble-counting. *Journal of Hydraulic Engineering* 136, 461-474.
775

776 Thomsen, K.J., Murray, A.S., Jain, M. and Bøtter-Jensen, L. 2008. Laboratory fading rates of
777 various luminescence signals from feldspar-rich sediment extracts. *Radiation Measurements*, 43,
778 1474–1486
779

780 Toms, P.S., Brown, A.G., Basell, L.S. and Hosfield, R.T. (2008) *Palaeolithic Rivers of south-*
781 *west Britain: Optically Stimulated Luminescence dating of residual deposits of the proto-Axe,*
782 *Exe, Otter and Doniford.* English Heritage Research Department Report Series, 2-2008.
783

784 Toms, P.S., Brown, A.G., Basell, L.S., Duller, G. and Schwenninger, J-L. (2013) *Chard Junction*
785 *Quarry, Somerset. Optical Stimulation Luminescence Dating of the Proto-Axe.* Scientific Dating
786 Report. English Heritage Research Department Report Series, no. 7-2013.
787

788 Wymer, J. J. 1999. The Lower Palaeolithic Occupation of Britain. Wessex Archaeology and
789 English Heritage, London.
790

791 Van Weert, F. H. A., van Gijssel, K., Leijnse, A., and Boulton, G. S. 1997. The effects of
792 Pleistocene glaciations on the geohydrological system of Northwest Europe. *Journal of*
793 *Hydrology* 195, 137-159.

794 Wenban-Smith, F. F. and Hosfield, R. T. (Eds.) 2001. *Palaeolithic Archaeology of the Solent*
795 *River*, Lithic Studies Occasional paper No. 7, London.

796 Westaway, R. 2002. Geomorphological consequences of weak lower continental crust, and its
797 significance for studies of uplift, landscape evolution, and the interpretation of river terrace
798 sequences. Netherlands. *Journal of Geosciences* 81, 283–304.

799 Westaway, R. 2010. Cenozoic uplift of southwest England. *Journal of Quaternary Science* 25,
800 419–432.
801

802 Westaway, R. 2011. Quaternary fluvial sequences and landscape evolution in Devon and
803 Somerset. In L. S. Basell, A. G. Brown and P. S. Toms (Eds.) *The Quaternary of the Exe Valley*
804 *and Adjoining Area. Field Guide. Quaternary Research Association, London, 27-46.*
805

806 Wright, J. F., Duchesne and Côté, M. M. 2003. Regional-scale permafrost mapping using the
807 TTOP ground temperature model. In Phillips, M., Springman, S.M. and Arenson, L.U. (Eds.)
808 *Permafrost*. Swets and Zeitinger, Lisse. 1241-1246.
809

810 Zaenetske, J. P., Gooseff, M. N., Bowden, W. B., Greenwald, M. J. and Brosten, T. R. 2008.
811 Influence of morphology and permafrost dynamics on hyporheic exchange in Arctic headwater
812 streams under warming climate conditions. *Geophysical Research Letters* 35, L02501.
813
814

815 **Tables**

816

817 Table 1. Dose Rate (D_r), Equivalent Dose (D_e) and Age data of samples from Hodge Ditch I-III
818 (51°N , 3°W , 75 m O.D.). Uncertainties in age are quoted at 1σ confidence, are based on
819 analytical errors and reflect combined systematic and experimental variability and (in
820 parenthesis) experimental variability alone. All ages are expressed in thousands of years before
821 2010.

822

823 Table 2. Pollen count data from large sub-sample from the Hodge Ditch III organic silty clay.

824

825 Table 3. Parameters used in TTOP modelling of permafrost freezing.

826

827

828 **Figure captions**

829

830 Fig. 1. (a) Location of the Axe valley catchment in southern England with catchments coded by
831 the number of BGS terraces recognised (after Brown et al., 2009) and ice limits , (b)
832 generalised geological section of the Jurassic Coast, (b) a simplified geological cross-section
833 along the Jurassic Coast with the Axe valley shown, and (c) a GIS derived drape of the
834 superficial geology of the Axe catchment. Data derived from BGS mapping.

835

836 Fig. 2. Drape of Quaternary deposits, archaeological (Palaeolithic) finds and sites mentioned in
837 the text over a DEM derived from IFSAR data.

838

839 Fig. 3. The long profile is re-drawn using some data from Campbell et al. (1998b), Basell et al.,
840 (2007), Brown et al. (2010) and this paper. Only the OSL dates with no analytical caveats are
841 plotted for CJQ. Upper stippling is Upper Greensand lithologies and below Triassic Mudstones
842 with the junction generalised from BGS mapping.

843

844 Fig.4. Generalised stratigraphic section from CJQ Hodge Ditch Phases 1-3 with insets of
845 sedimentological features (a) upper diamicton unit, (b) organic-rich clay in upper part of Unit
846 B, (c) channel sands with frost cracks between unit B and C, (d) sand lenses within Unit C, (e)
847 clast-supported horizontally bedded gravels in Unit C, (f) a sarsen from Unit B showing surface
848 weathering pits, (g) the brecciated and disrupted bedrock-gravels interface in Hodge Ditch II.

849

850 Fig. 5. Scanned face of a section in with Scan data draped Hodge Ditch 3 with photos taken
851 using the ScanStation and then processed using different image texture settings (upper gamma
852 2 and lower using a colour classification of the intensity of return).

853

854 Fig. 6. (A) HD I, II and III point data interpolated in ArcMap 10 using inverse distance eighting
855 and displayed using height colour values. Displayed in ArcMap (2D) using a pseudo-3D image.
856 Red high, blue low. Red points show distribution of OSL locations labelled according to GL-
857 number. (B) Model with OSL sample locations (black), bedrock from bore hole data, location
858 of one of the scanned faces (pale mauve) inserted from scanned grid co-ordinates as an
859 example, palaeosol (bright pink line in HD3) and location of major sand units derived from
860 scan data and photographs. Artefact locations are shown in bright pink. The apparent position
861 of some of the OSL sample locations within mounds of gravel is because following standard
862 gravel extraction during which samples were taken and sections recorded, the area was

863 subsequently used to dump spoil mounds which were captured by a later scan. 5 x vertical
864 exaggeration.

865

866 Fig. 7. Age depth model derived from OSL and bio-correlation dates. Solid red line signifies the depth
867 of the thin palaeosol. Dashed grey line indicates the level at which artefacts were found. Diamonds
868 represent OSL age estimates, with red fill used to highlight those with analytical caveats. The blue line
869 shows the oxygen isotope curve from ODP 677 along with temperate (red numbered) and cool (blue
870 numbered) MIS.

871

872 Fig. 8. Grains size envelope for CJQ fluvial gravels from Hodge Ditch I-III with moment
873 statistics and size range of the bifaces found during this research.

874

875 Fig.9. GIS DEM of the mapped area around the CJQ showing spring-related thaw-slump
876 landforms (marked by break of slopes as mapped and by symbols A-E). The map uses standard
877 geomorphological symbols as recommended by the Geological Society Engineering Working
878 Party (1972) and reproduced in Gardiner and Dackombe (1983).

879

880 Fig. 10. Simplified model of para-fluvioperiglacial sediment input forced by permafrost
881 melting of the Upper Cretaceous (Greensand) lithological sequence, (a) model representation,
882 (b) the valley-side cross-sectional geology used in the model with present water table and (c)
883 the model with frozen layer and flowlines after sequential melting.

884

885

886

887

888

Fig 1

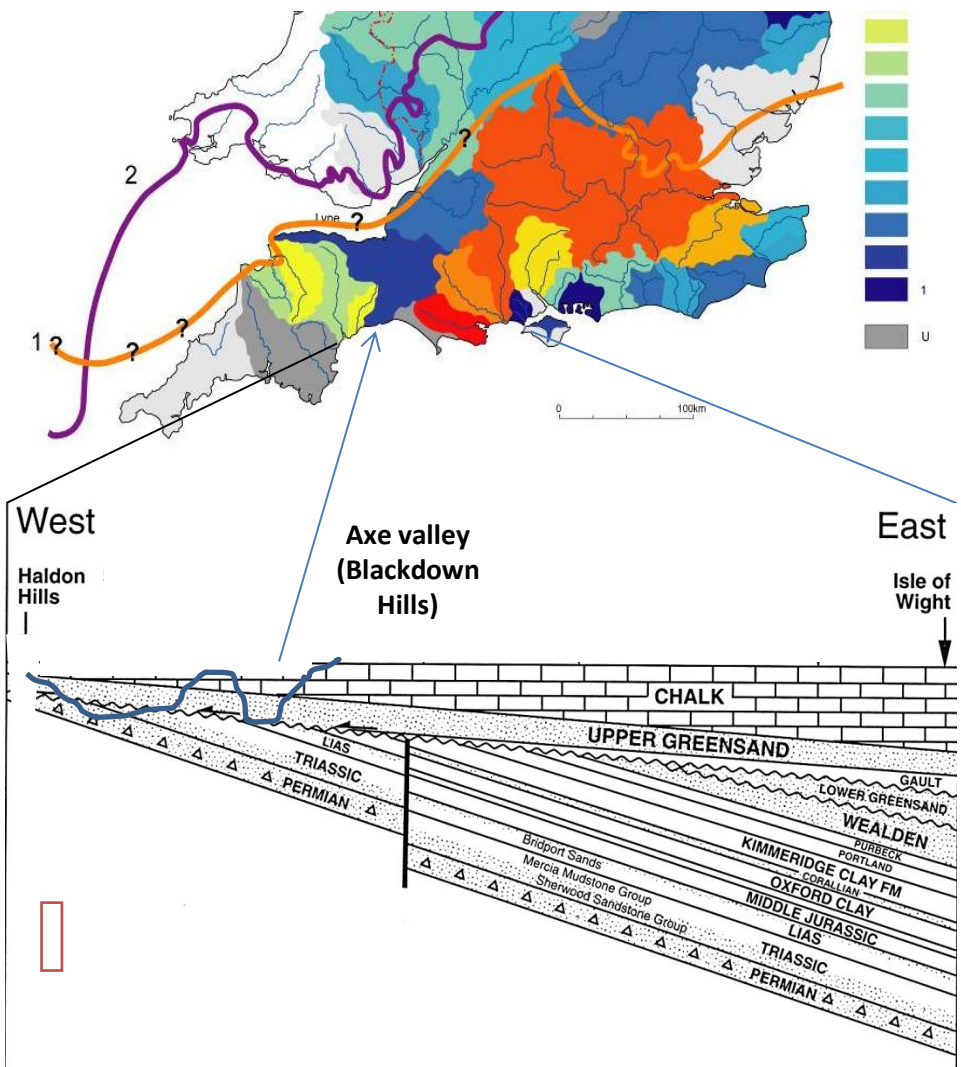


Fig 2

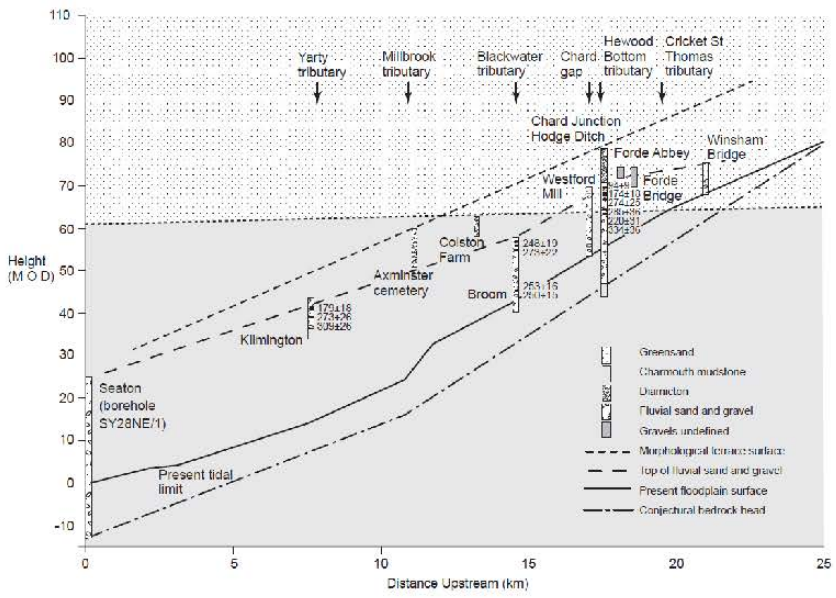


Fig 3

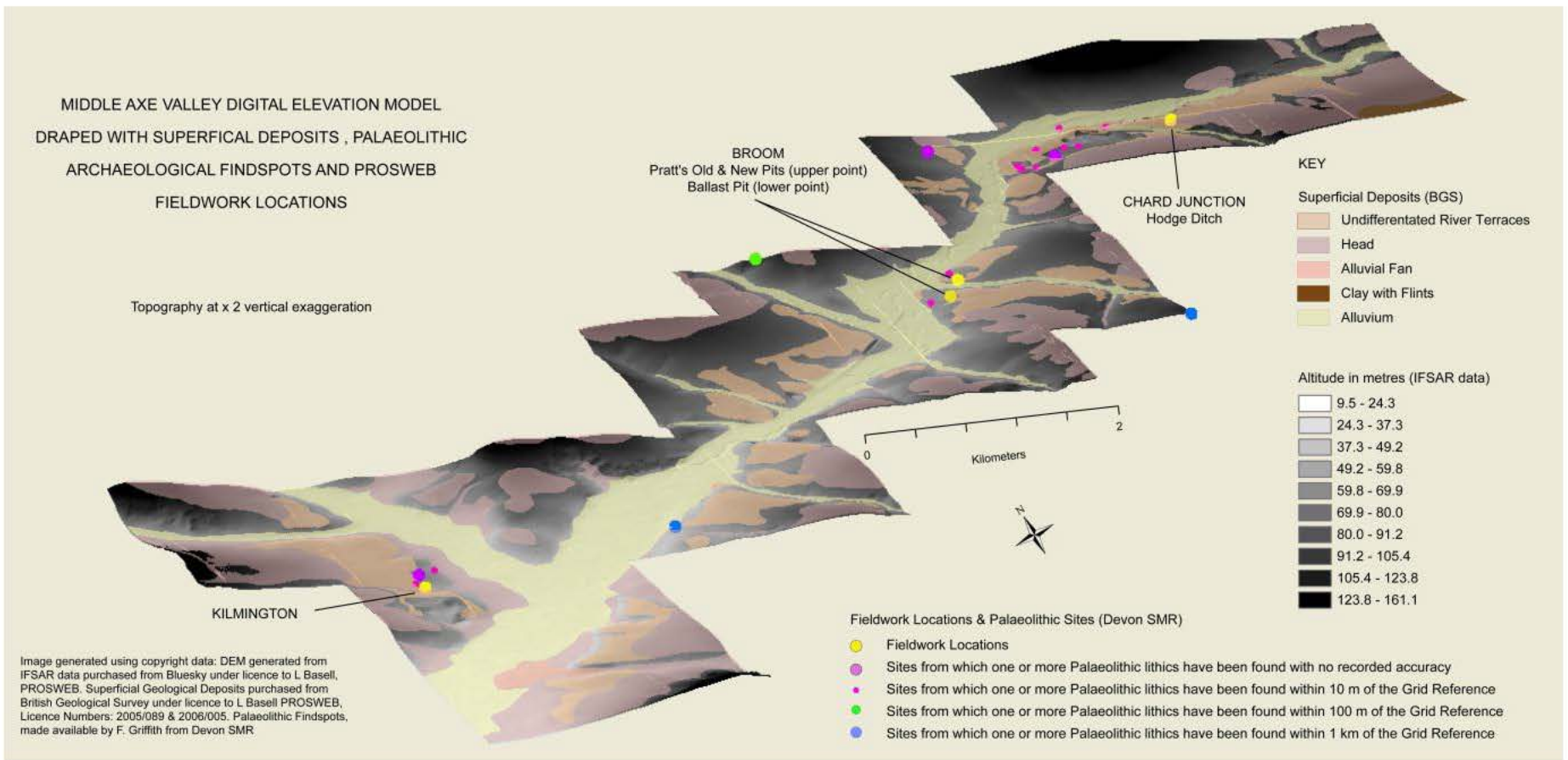
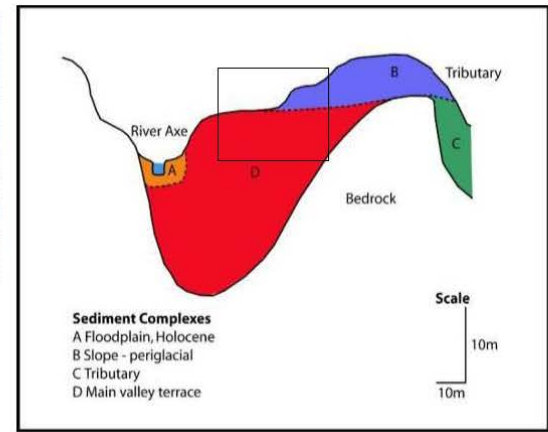
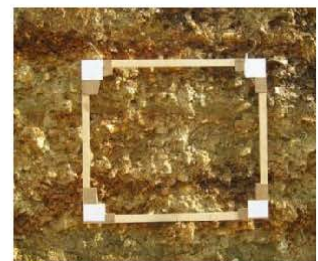
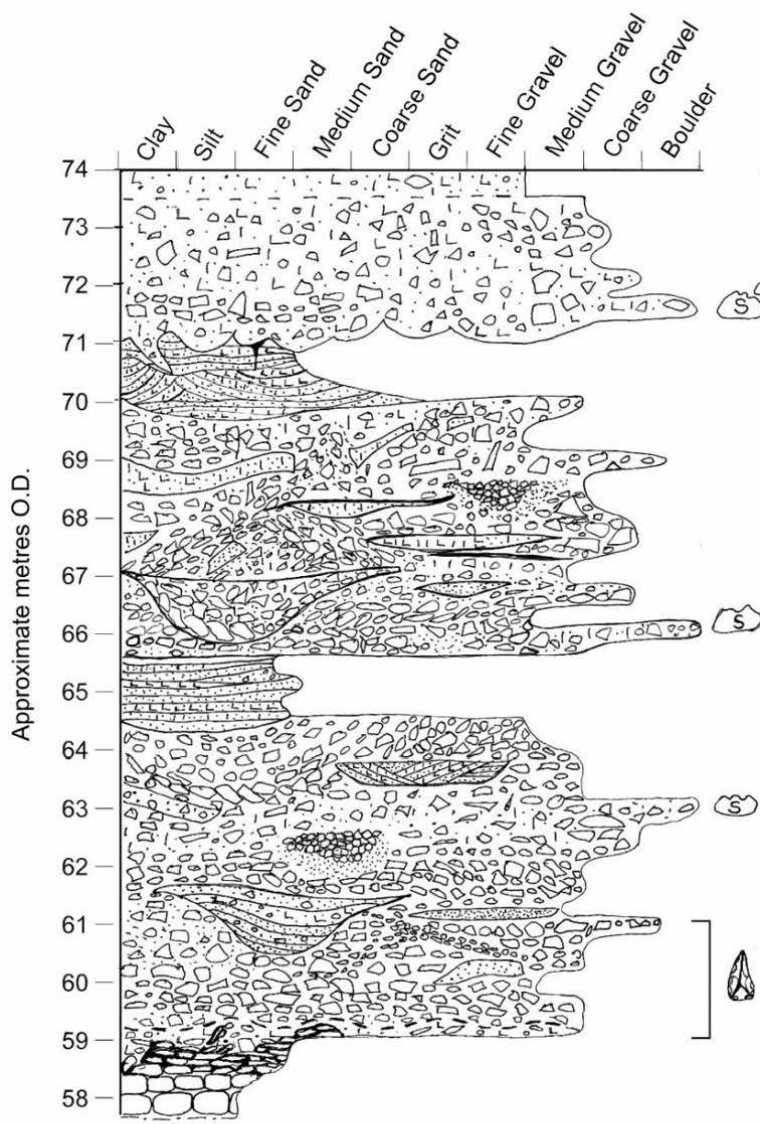


Fig 4



- | | | | |
|------|------------------|-------------|--|
| Clay | Clay drape | Bifaces | Weathered Charmouth Mudstone, Gravel, Sand, Silt, & Clay |
| Silt | Diffuse boundary | Sarsens | |
| Sand | Framework Gravel | Frost Crack | Charmouth Mudstone |

Fig 5

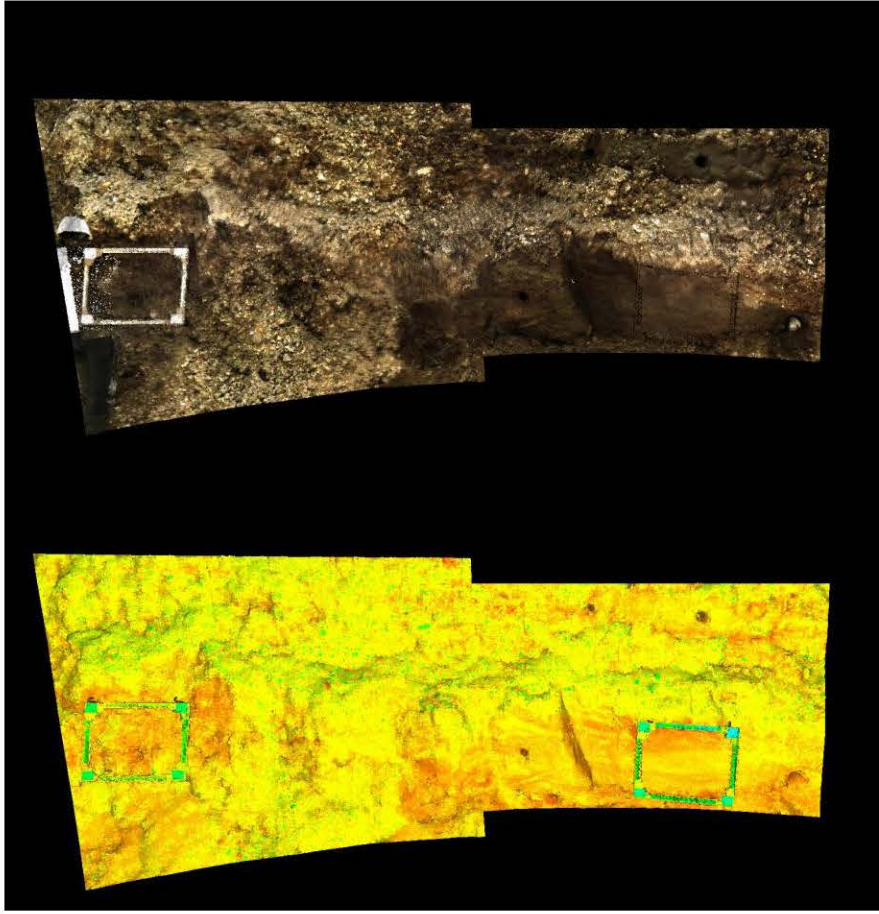
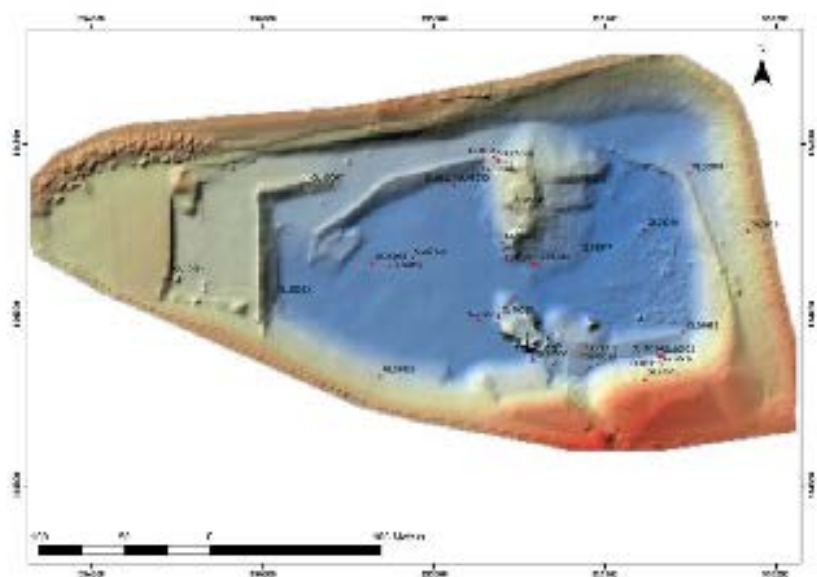


Fig 6

A



B

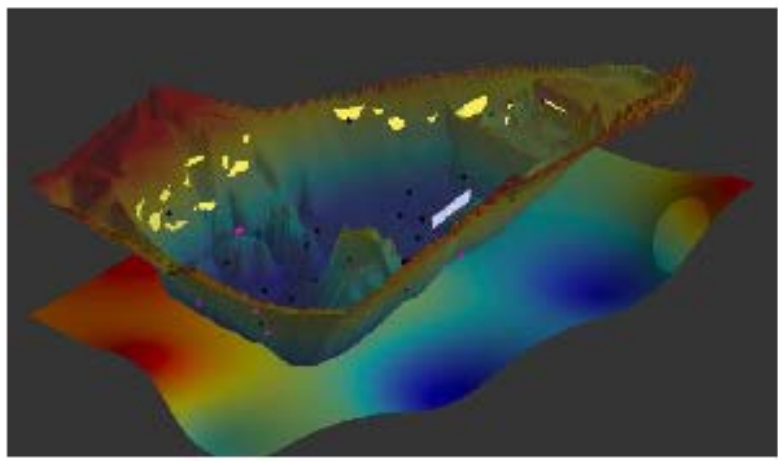


Fig 7

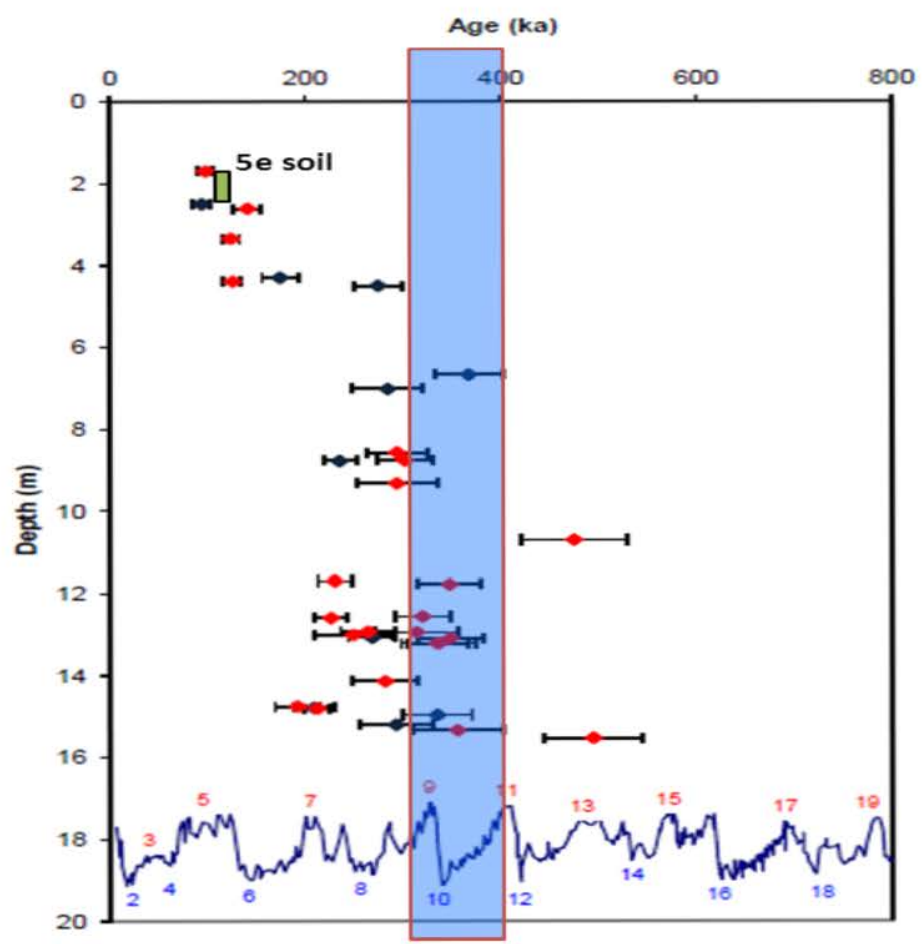


Fig 8

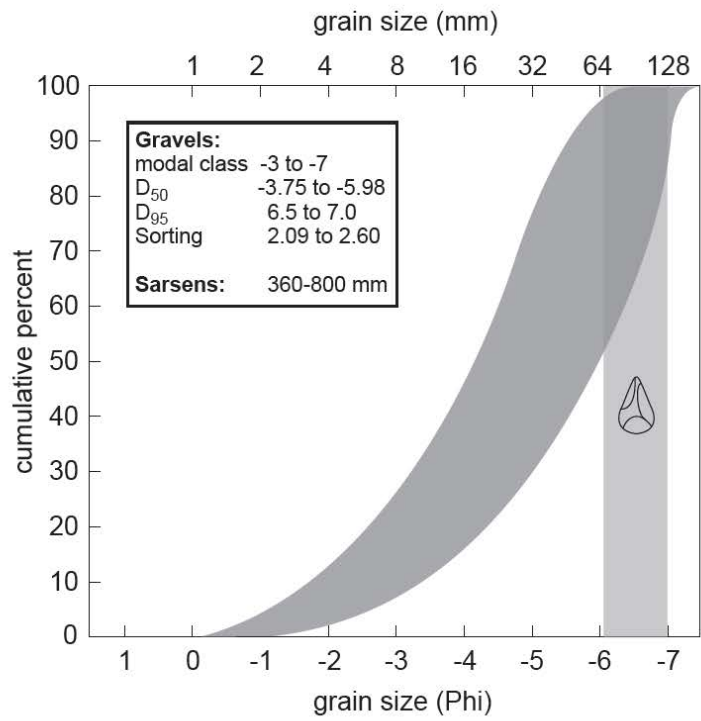
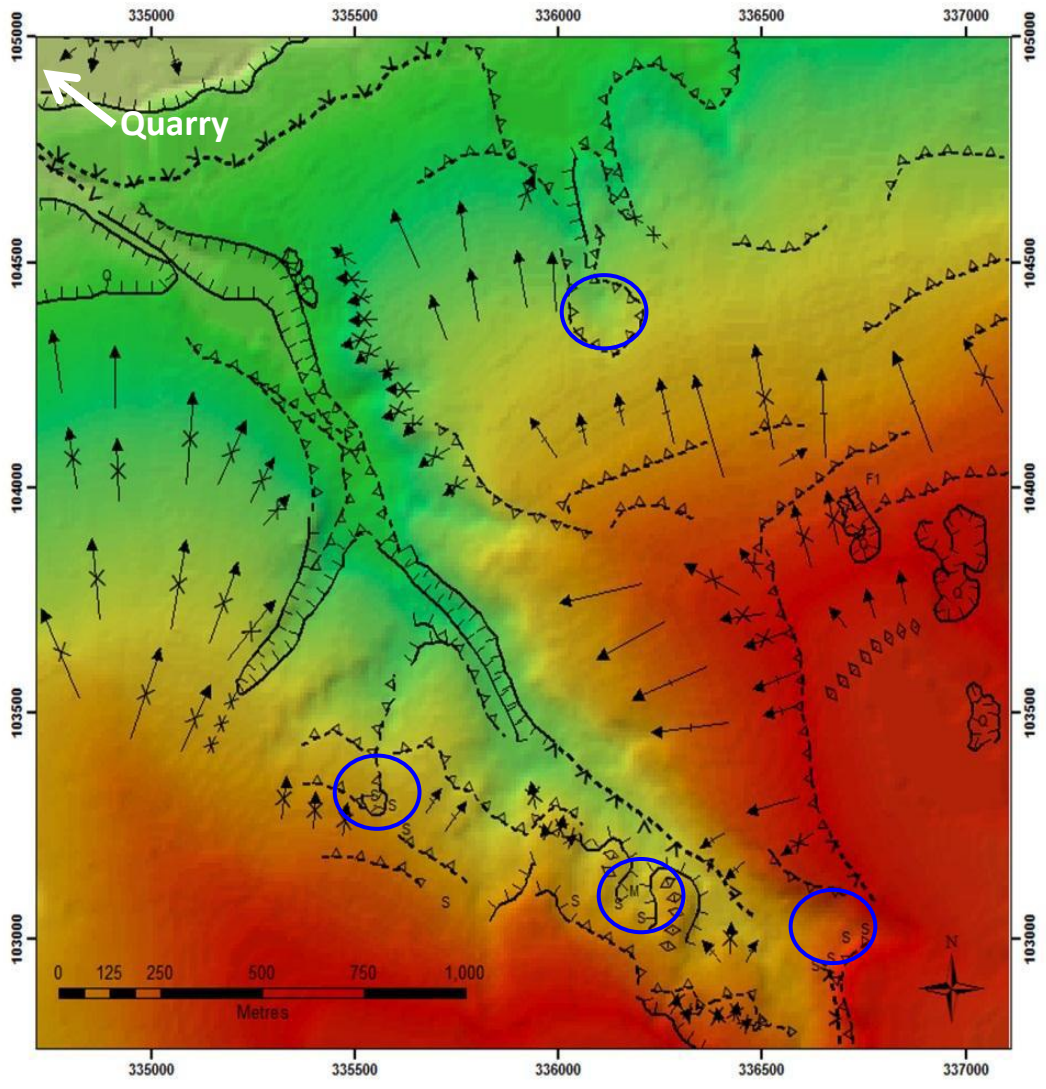


Fig 9



Legend

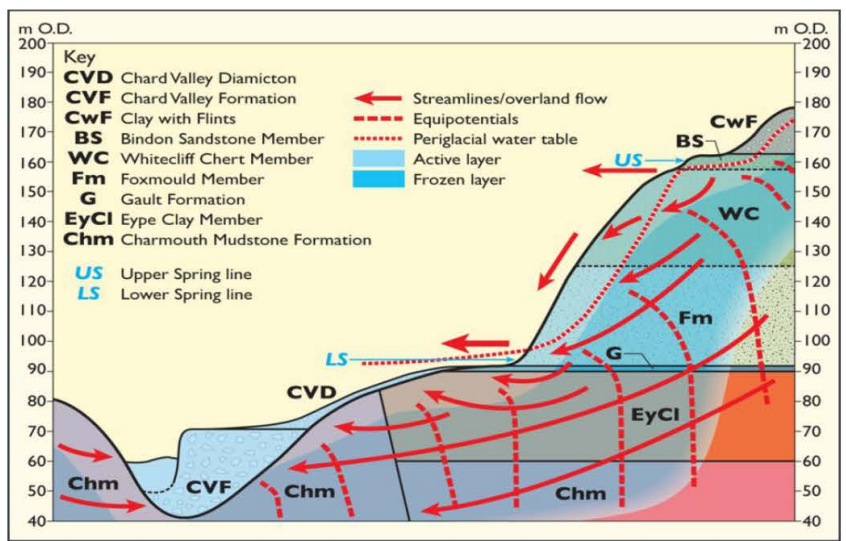
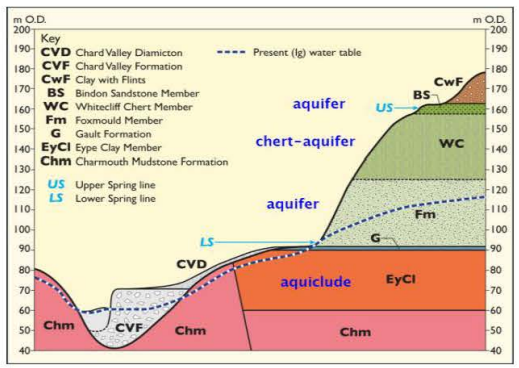
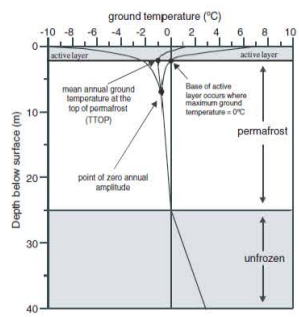
- |> Concave slope unit
- > Rectilinear slope unit
- |< Convex slope unit
- -v- Smooth change of slope, concave
- |—| Abrupt break of slope
- △-△ Smooth change of slope, convex
- ◇◇◇ Rounded ridge crest
- *-* Rounded valley axis

Background

Shaded Relief DTM of
Digimap Ordnance
Survey Landform Profile Data
1:10,000 under licence to
University of Southampton.
Displayed as RGB.
High (279 m) and low
(13.7 m) values
determined by raster extent.

- Q = Quarry
- S = Spring
- M = Spring Mire
- F1 = Lithic Find 1

Fig 10



Lab Code	Overburden (m)	Grain size (µm)	Moisture content (%)	α D _r (Gy.ka ⁻¹)	β D _r (Gy.ka ⁻¹)	γ D _r (Gy.ka ⁻¹)	Cosmic D _r (Gy.ka ⁻¹)	²²⁶ Ra/ ²³⁸ U	Total D _r (Gy.ka ⁻¹)	Preheat (°C for 10s)	D _e (Gy)	Age (ka)
GL06010	4.3	125-180	16 ± 4	-	1.09 ± 0.10	0.34 ± 0.02	0.11 ± 0.01	1.25 ± 0.27	1.54 ± 0.10	240	268.5 ± 22.0	174 ± 18 (16)
GL06011	2.5	125-180	13 ± 3	-	0.53 ± 0.04	0.29 ± 0.01	0.14 ± 0.01	0.76 ± 0.12	0.96 ± 0.05	260	90.2 ± 6.8	94 ± 9 (7)
GL06012	1.7	125-180	14 ± 3	-	1.28 ± 0.11	0.53 ± 0.02	0.16 ± 0.02	1.07 ± 0.22	1.97 ± 0.11	260	193.7 ± 11.0	98 ± 9 (6) ^{a,b}
GL06013	4.5	125-180	15 ± 4	-	0.72 ± 0.07	0.26 ± 0.01	0.10 ± 0.01	0.96 ± 0.25	1.09 ± 0.07	240	298.6 ± 19.2	274 ± 25 (20)
GL06057	6.7	125-180	16 ± 4	-	0.75 ± 0.07	0.20 ± 0.01	0.08 ± 0.01	1.04 ± 0.17	1.02 ± 0.07	240	375.3 ± 24.6	367 ± 35 (29)
GL06058	7.0	125-180	15 ± 4	-	0.84 ± 0.08	0.21 ± 0.01	0.07 ± 0.01	0.78 ± 0.12	1.12 ± 0.08	280	318.3 ± 33.3	284 ± 36 (32)
GL08043	15.3	125-180	17 ± 4	-	0.54 ± 0.05	0.22 ± 0.01	0.03 ± 0.00	0.88 ± 0.16	0.80 ± 0.6	280	284.9 ± 31.9	355 ± 47 (43) ^c
GL08044	15.2	125-180	21 ± 5	-	1.22 ± 0.13	0.38 ± 0.02	0.03 ± 0.00	1.03 ± 0.14	1.63 ± 0.14	280	477.2 ± 45.1	292 ± 37 (33)
GL08045	12.9	125-180	17 ± 4	-	0.97 ± 0.09	0.26 ± 0.01	0.03 ± 0.00	0.99 ± 0.16	1.26 ± 0.10	280	332.7 ± 23.8	264 ± 28 (23) ^c
GL08046	15.0	125-180	20 ± 5	-	1.04 ± 0.11	0.48 ± 0.02	0.03 ± 0.00	1.00 ± 0.12	1.56 ± 0.11	260	521.4 ± 41.5	334 ± 36 (31)
GL08047	15.5	125-180	20 ± 5	-	1.03 ± 0.11	0.42 ± 0.02	0.03 ± 0.00	0.79 ± 0.09	1.49 ± 0.11	280	736.8 ± 51.7	494 ± 50 (43) ^{c,d}
GL09029	3.3	125-180	13 ± 3	-	0.54 ± 0.05	0.41 ± 0.02	0.12 ± 0.01	0.87 ± 0.16	1.07 ± 0.05	260	132.1 ± 7.0	124 ± 9 (7) ^e
GL09030	8.1	125-180	13 ± 3	-	0.53 ± 0.05	0.22 ± 0.01	0.06 ± 0.01	0.87 ± 0.22	0.82 ± 1.43	250	247.4 ± 18.9	302 ± 29 (25) ^c
GL09031	9.6	125-180	15 ± 4	-	1.09 ± 0.10	0.28 ± 0.01	0.05 ± 0.01	0.91 ± 0.12	1.43 ± 0.10	230	419.8 ± 31.7	294 ± 30 (26) ^c
GL09117	11.8	5-15	21 ± 5	0.38 ± 0.04	1.44 ± 0.14	0.81 ± 0.03	0.04 ± 0.00	1.21 ± 0.14	2.67 ± 0.15	210	928.1 ± 64.8	347 ± 31 (28) ^d
GL09118	11.7	5-15	19 ± 5	0.35 ± 0.04	1.48 ± 0.14	0.79 ± 0.03	0.04 ± 0.00	0.83 ± 0.10	2.67 ± 0.15	250	614.0 ± 30.6	230 ± 17 (14) ^d
GL09119	8.8	5-15	19 ± 5	0.35 ± 0.04	1.23 ± 0.12	0.61 ± 0.02	0.06 ± 0.01	1.07 ± 0.14	2.26 ± 0.12	260	529.9 ± 24.5	235 ± 17 (14)
GL09120	10.7	125-180	8 ± 2	-	0.59 ± 0.04	0.24 ± 0.01	0.05 ± 0.00	0.90 ± 0.16	0.88 ± 0.05	240	419.1 ± 41.5	475 ± 53 (48) ^e
GL10001	2.6	180-250	9 ± 2	-	0.57 ± 0.04	0.46 ± 0.02	0.14 ± 0.01	0.88 ± 0.14	1.17 ± 0.05	280	164.9 ± 15.6	141 ± 14 (14) ^b
GL10002	13.1	180-250	13 ± 3	-	0.51 ± 0.05	0.31 ± 0.02	0.04 ± 0.00	1.05 ± 0.24	0.86 ± 0.05	240	229.4 ± 16.2	268 ± 25 (21)
GL10013	13.1	125-180	21 ± 5	-	0.50 ± 0.05	0.27 ± 0.01	0.04 ± 0.00	0.96 ± 0.30	0.80 ± 0.06	240	279.4 ± 18.0	348 ± 34 (14) ^c
GL10014	12.9	125-180	12 ± 3	-	0.56 ± 0.05	0.31 ± 0.02	0.04 ± 0.00	0.97 ± 0.25	0.91 ± 0.05	260	284.4 ± 34.1	313 ± 42 (21) ^b
GL10015	14.7	125-180	16 ± 4	-	1.02 ± 0.10	0.50 ± 0.02	0.03 ± 0.00	1.13 ± 0.16	1.55 ± 0.10	260	298.3 ± 30.2	192 ± 23 (40) ^b
GL10016	14.8	125-180	18 ± 4	-	0.84 ± 0.08	0.37 ± 0.02	0.03 ± 0.00	0.98 ± 0.13	1.24 ± 0.09	260	257.7 ± 19.0	208 ± 21 (44)
GL10019	13.0	125-180	15 ± 4	-	0.82 ± 0.08	0.20 ± 0.01	0.04 ± 0.00	0.99 ± 0.17	1.06 ± 0.08	240	262.5 ± 37.9	249 ± 40 (38) ^c
GL10020	14.1	125-180	15 ± 4	-	0.92 ± 0.08	0.35 ± 0.02	0.03 ± 0.00	0.93 ± 0.12	1.30 ± 0.09	240	366.8 ± 37.2	281 ± 34 (31) ^{b,c}
GL10055	13.2	125-180	6 ± 2	-	0.52 ± 0.04	0.28 ± 0.01	0.04 ± 0.00	-	0.84 ± 0.04	260	281.7 ± 21.2	335 ± 31 (26) ^b
GL10063	12.6	125-180	19 ± 5	0.32 ± 0.04	1.33 ± 0.13	0.17 ± 0.01	0.04 ± 0.00	0.98 ± 0.12	1.85 ± 0.13	240	592.7 ± 38.5	320 ± 31 (27)
GL10064	14.8	125-180	11 ± 3	-	0.56 ± 0.05	0.26 ± 0.01	0.03 ± 0.00	0.95 ± 0.24	0.85 ± 0.05	240	180.4 ± 9.5	212 ± 17 (13) ^c
GL10065	12.6	125-180	17 ± 4	-	0.78 ± 0.08	0.41 ± 0.02	0.04 ± 0.00	0.98 ± 0.19	1.24 ± 0.08	240	280.0 ± 17.5	226 ± 20 (17) ^c
GL10066	13.2	125-180	17 ± 4	-	1.11 ± 0.12	0.72 ± 0.08	0.04 ± 0.00	1.17 ± 0.16	1.87 ± 0.15	240	627.2 ± 58.1	336 ± 42 (38) ^{a,d}
GL10067	9.3	125-180	17 ± 4	-	0.98 ± 0.09	0.27 ± 0.01	0.06 ± 0.01	1.01 ± 0.16	1.31 ± 0.10	240	384.8 ± 50.1	293 ± 44 (41) ^c
GL10084	4.4	125-180	19 ± 5	-	0.62 ± 0.05	0.49 ± 0.02	0.10 ± 0.01	1.01 ± 0.16	1.21 ± 0.06	240	152.1 ± 10.4	126 ± 11 (9) ^a

Analytical Caveats: ^aSignificant feldspar contamination, ^bFailed dose recovery test, ^cFailed repeat dose ratio test, ^dD₀ exceeds 600 Gy, ^ePotential partial bleaching, ^fLimited sample mass